

# **MICROFABRICATED DYNAMIC SHAPE-CHANGE HYDROGEL SYSTEMS**

by  
Tanvi Shroff

A thesis submitted to Johns Hopkins University in conformity with the requirements for the  
degree of Master of Science in Engineering

Baltimore, Maryland

May, 2016

© 2016 Tanvi Shroff

All Rights Reserved

## **ABSTRACT**

Biomimicry is gaining traction in the engineering community to create simple, elegant designs and constructions. Combining this with the microfabrication skills that the semiconductor industry has perfected, has enabled researchers to create high throughput, cost effective solutions to major challenges in the study of soft material dynamics.

This thesis provides an insight into the possibilities that come with understanding the mechanics behind fast movements in the plant kingdom, and origami, to create systems that exhibit bidirectional folding using microfabrication. A thermoresponsive hydrogel sheet was fabricated, with stiffer non-swelling polymer grids embedded in it, which was the basis for its self-folding properties and behavior. In addition to this, a gut parasite inspired system was introduced, which could potentially give rise to a new type of adhesive drug delivery devices. Microfabrication skills such as photolithography were used to a large extent, to photopattern thermoresponsive hydrogels like poly (N-isopropyl acrylamide) and mucoadhesive materials like chitosan. The drug release kinetics for this model was assessed, and future steps proposed, to make this a viable adhesive system.

Advisor: Dr. David Gracias

Reader: Dr. Rebecca Schulman

## ACKNOWLEDGMENTS

I would like to thank Dr. Gracias for giving me the opportunity to pick a topic that interested me, and encouraging me to make the most of my time here. His “figure it out as long as you don’t break anything” style of mentoring taught me that I can be an independent researcher, knowing that I could rely on him to brainstorm with me in tough situations. I found very reliable friends in the Gracias Lab, who made my time here more memorable. I also found a mentor in my collaborator, Dr. Nguyen and I would like to thank her and her lab for all her support. I also sincerely thank Dr. Schulman, for agreeing to be a reader for this thesis.

Dr. Goffin and Dr. Pereira were great mentors and gave me the opportunity to TA, which caused me to now have a newfound respect for the teachers I had throughout my academic career. I would like to thank the staff at the Chemical & Biomolecular Engineering for always being around to keep me more informed about the daily workings of the department. Another thank you to my mentors and all my professors at Hopkins, I am grateful to have had the chance to interact with them.

The Master’s program at JHU brought me to a new continent, filled with new experiences and perspectives. In these dynamic times, the love of my family, friends back home and alma mater stayed, unwavering. A sincere thank you to my parents, grandparents and siblings for always making me smile, reminding me of how far I have come, and calming me down when I talked about how I had miles before I went to sleep.

Last but not least, I have my entire support system at Hopkins, in the form of all the friends I had over the last two years, they set the bar high for all my future acquaintances.

## TABLE OF CONTENTS

ABSTRACT.....	ii
ACKNOWLEDGMENTS .....	iii
TABLE OF CONTENTS.....	iv
FIGURES.....	v
TABLES.....	viii
CHAPTER 1. INTRODUCTION .....	1
1.1.    Lithography to create three-dimensional structures .....	1
1.2.    Self-folding systems with differentially swelling hydrogel actuators .....	4
1.3.    Nature undergoes bidirectional folding .....	7
1.4.    Stimuli responsive materials .....	9
CHAPTER 2. REVERSIBLE BIDIRECTIONAL FOLDING OF A HYDROGEL SYSTEM.....	13
2.1.    Introduction .....	13
2.2.    Fabrication and experiments .....	20
2.3.    Results and Discussions .....	24
2.4.    Applications and Future Steps.....	36
CHAPTER 3. SCOLEX-INSPIRED DRUG DELIVERY SYSTEM.....	40
3.1.    Introduction .....	40
3.2.    Fabrication and Experiments .....	48
3.3.    Results and Discussions .....	56
CHAPTER 4. SUMMARY AND FUTURE STEPS .....	60
REFERENCES .....	61
CURRICULUM VITAE .....	76

## FIGURES

Figure 1 - A schematic of the ways a polymer system can bend out of plane. a.) Bilayer of polymers that undergo differential swelling, b.) Laterally arranged polymers that undergo differential swelling, c.) Polymer with a crosslinking gradient along its thickness, d.) Incorporation of a trigger layer that can be eliminated to cause bending of the strained bilayer underneath. Reprinted with permission from Ref. [36] © 2013, Current Opinion in Chemical Engineering.....	5
Figure 2 - The actions involved in a Venus Flytrap snapping shut to catch its prey. Image obtained from <a href="http://www.naturalhistorymag.com/biomechanics/112001/snap">http://www.naturalhistorymag.com/biomechanics/112001/snap</a> .....	13
Figure 3 - The changes in the orientation of a Venus Flytrap leaf in action, when closing on prey. The orientation of the leaf changes from concave when open to convex when closed. Reprinted with permission from Ref. [49] © 2005, Nature. ....	14
Figure 4 - Miura ori pattern can be created using origami, contains interrelated folds that allow the entire sheet to be folded into a compact form by the application of a unidirectional force. Image obtained from <a href="http://www.origami-resource-center.com/origami-science.html">http://www.origami-resource-center.com/origami-science.html</a> .....	15
Figure 5 - Miura ori employed in the design of a telescopic lens, that can be packed onto a satellite and unfolded in space, at the time of need, once the satellite has safely been incorporated into orbit. Image obtained from <a href="http://www.origami-resource-center.com/origami-science.html#eyeglass">http://www.origami-resource-center.com/origami-science.html#eyeglass</a> .....	15
Figure 6 - Folding of a prestressed polystyrene sheet at the hinges, which are black lines printed on the sheet, which attain glass transition temperature before the unmarked regions of the sheet. Reprinted with permission from Ref. [88] © 2012, Soft Matter .....	17
Figure 7 – A schematic of the bidirectional folding capability of the thermoresponsive hydrogel system .....	19
Figure 8 - Top view of the bidirectional folding hydrogel system design, with dimensions. The blue region represents the hydrogel sheet while the white rectangles are the grids of non-swelling SU-8 photoresist. The spacing between the grids varies as: $a = 500\ \mu\text{m}$ , $b = 400\ \mu\text{m}$ .....	20
Figure 9 - Negative masks for the hydrogel system. a. SU-8 mask for the stiff non swelling grids, b. rectangular shape for the pNIPAM layer of the hydrogel system. ....	21

Figure 10 - Microfabrication schematic of the hydrogel and grid system.....	21
Figure 11 - Liftoff of shapes from the wafer, the last step of the fabrication process to show how the shapes naturally curl concave along the short side. The beads roll off the surface, proving this. ....	25
Figure 12 - Bidirectional folding schematic with images from experimentation .....	25
Figure 13 - Images from the bidirectional folding experiments, the leftmost image is the beginning of a warmup phase, the image in the middle shows the flat state in transition, the image on the right shows the shape at the end of the warmup phase. The red arrows indicate the warmup phase, the blue arrows indicate the cooldown phase. Scale bars: 1 cm. ....	26
Figure 14 – (Left) Mask of the systems to be studied for bidirectional folding dependence on aspect ratio. Of the SU-8 mask on the left, the bottom three shapes indicate the original system with SU-8 grid aspect ratio = 2.375:1. The square grids indicate 1:1 aspect ratio, of side length = 800 $\mu\text{m}$ and the remaining grids are of aspect ratio 1:2.375. (Right) pNIPAM masks corresponding to the SU-8 masks.....	27
Figure 15 – (left) investigating the onset of bidirectional folding by varying the number of rows and columns of SU-8 grids. (Right) The pNIPAM masks corresponding to the SU-8 masks.....	30
Figure 16 - (left) SU-8 masks to study the dependence of bidirectional folding on square grid dimensions. (Right) the pNIPAM masks corresponding to the SU-8 masks.....	31
Figure 17 - 200 $\mu\text{m}$ grids, the left figure shows the shape in the cold state, while the figure on the right shows the shape in the warm state, which exhibits uneven curling. Scale bars: 1 cm .....	33
Figure 18- Proof of bending in each grid of the hydrogel grid system .....	34
Figure 19 - A visualization of the gold plated hydrogel - grid system, with respect to the silicon wafer (grey) in the absence of the sacrificial layer. The red layer below the yellow SU-8 layer is the gold layer, while the blue layer is the pNIPAM layer.....	35
Figure 20 - The bidirectional folding system as a thermoresponsive cargo offloading device. Scale bar: 1 cm .....	38
Figure 21 - The bidirectional folding system represented as a thermoresponsive photovoltaic. Scale bar: 1 cm. ....	38
Figure 22 - The components and characteristics of an effective drug delivery system.	
Reprinted with permission from Ref. [26] © 2012, Advanced Drug Delivery Reviews.....	41

Figure 23 - Adhesion mechanism of octopus suckers. . Reprinted from Ref. [141]© 2013, PLoS ONE.....	47
Figure 24 - An image of the suction cup, after the liftoff step of fabrication. (a.) A side view of the suction cup at room temperature, observed using bright field microscopy, (b.) the top view of the suction cup at room temperature, using bright field microscopy, (c.) side view of the room temperature suction cup, using fluorescence imaging (d.) Indicates the side view of the collapsed suction cup in warm water. The red arrow indicates warming while the blue arrow indicates cooling.....	51
Figure 25 - Microfabrication schematic for the suction cups .....	52
Figure 26 – (a.) Spokes in the SU-8 mask of 50 $\mu\text{m}$ thickness, (b.) The system after liftoff, once the pNIPAM layer is swollen.....	53
Figure 27 – (a.) A mask of another system of SU-8 mimicking the circular muscles, which contains a rim of SU-8 and a central patch of 200 $\mu\text{m}$ diameter. (b.) The system after liftoff, when the pNIPAM layer is swollen.....	53
Figure 28 - (Top) The correlation between the fluorescence counts measured from the plate reader as a function of the concentration of fluorescein in mg/ml released into the warm water. (Bottom) The dye release studies for the suction cups in warm water in comparison to the control, of suction cups in water at room temperature. ....	55
Figure 29 - Photopatterning a mucoadhesive based on chitosan and polyacrylic acid.....	58

## TABLES

Table 1 - Results of bidirectional folding for shapes with aspect ratio 2.4:1 (3 viable samples)	
.....	26
Table 2 - Results of the bidirectional folding experiment for the shapes with aspect ratio 1:1 (4 viable samples). ....	28
Table 3 - Bidirectional folding experiment results for samples with aspect ratio 1: 2.4 (5 viable samples). ....	28
Table 4 - Effect of varying the no. of rows and columns, on bidirectional folding.....	30
Table 5 - The dependence of bidirectional folding on the size of the square grids .....	32



## CHAPTER 1. INTRODUCTION

### 1.1. Lithography to create three-dimensional structures

Lithography, a process of fabrication fundamental to the semiconductor industry, is a low cost, high throughput process of creating numerous semiconductor devices simultaneously. This is a very efficient method of creating articles on a substrate, up to a very high resolution with a reasonably high yield, crucial to the creation of microelectromechanical systems (MEMS), microreactors, sensors and antennae.[1]–[5]

One way to create 3D structures using lithography is to create 2-D designs of shape with components having characteristics that could respond to certain stimuli, like temperature, light, pH, presence of aqueous media, and relying on the principles governing self-assembly and self-folding to bring the components together into a three-dimensional final structure. Some cases of this folding can be a form of mesoscale self-assembly, where components of a 3-D shape are pieced together from their disassembled components.[6], [7] This differs from microscale self-assembly where nanocomponents and molecules come together to create a larger structure like a crystal or multifunctional surface.[8] Instances of millimeter self-folding come from an article by Boncheva et al., who review the methods to create millimeter scale objects, one of the applications of which involves fabrication of 3-D structures using 2-D fabrication techniques, upon imparting a stimulus to cause the folding.[9] These characteristics might allow certain components of the shapes to respond to the stimuli, creating stresses or changes in swelling patterns and to cause the whole shape to fold out of plane to minimize the energy of the system and to attain a new steady state conformation in a three dimensional plane. There are also cases when the 3-D folding can be brought about by capillary forces and surface tension, where the final shape can be controlled by the initial 2-D shape, and the rate

of liquid evaporation and thus the high surface tension which pulls the sides of the shape up into a 3D plane.[10],[11]

The Gracias Lab has employed materials with lower melting points to be hinges for 2-D patterned shapes of dismantled boxes. Upon heating, the hinge materials melt and ball up trying to minimize surface tension, and tend to pull the different faces of the boxes together, to create cubes and other encapsulation mechanisms.[12] This can be used to create other kinds of polyhedral, and the surface tension of the hinge materials leads to the creation to complex shapes.[13] They have also reported self-folding biopsy tools for cell or tissue capture, made of magnetically controllable metals, whose direction can be manipulated by a magnetic field.[14]

Encapsulation mechanisms are employed for drug delivery as well, where macromolecules or drug molecules can be enclosed within the device, which can be released in a systematic and timely fashion. Current technology in drug encapsulation exists in the form of polymer capsules, liposomes, nanoparticle systems and other micro-engineered systems.[15]–[25] The reason to incorporate the molecule of choice into an encapsulation system may be to increase targeting towards a particular site in the body, enhance prolonged release of the therapeutic agent, reduce the side effects of a drug or to improve the solubility of a drug substance.

Similar encapsulation mechanisms in the form of hollow boxes and prisms were created using photolithography of hydrogels, where the folding was brought about by a crosslinking gradient and hence differential swelling of the hydrogel in an aqueous environment.[26] A review by Ionov investigates the design of various self-folding hydrogel films and the stimuli that they could respond to.[27] Yoon et al employed a thermoresponsive

polymer, pNIPAM (poly(N-isopropyl acrylamide)), to create self-folding hydrogel boxes and cargo carriers.[28], [29] In these cases a UV-induced crosslinking gradient leads to differential absorption of water by the gel, which in turn drives curling. A similar study was carried out by Jamal et al to create self-folding microfluidics. They were inspired by the folded channel in plant leaves, which act as natural microfluidic channels in a 3-D realm. They were able to create curling SU-8 channels and structures by the introduction of a crosslinking gradient because of the direction in which the UV light was shined on the spincoated SU-8 substrate. The incorporation of the crosslinking gradient led to varying levels of crosslinking in the polymer and hence, varying extents of water absorption and retention, which led to those regions curling more than others.[30]

Brittain et al detail a method to create 3-D folding structures inspired by origami involving 2-D microfabrication techniques like etching and micro-contact printing. They created a geometric imprint of a temporary mask of a thiol on a surface of a silver coated substrate. This enabled selective etching of the region of the substrate, not covered by the mask. Upon manual removal of the unetched region, the alignment of the individual sections of the shape could fold owing to differences in the thickness of the structure. The pattern of the etching was inspired by origami and caused the shape to fold into many forms like arches and birds. Electrodepositing a layer of a structural material can consolidate this folded structure.[31] Epstein et al create elastic instability-driven shape changing colloidal particles which undergo a snap buckling behavior in the presence of increasing pH which increases the mismatch in strain.[32]

## **1.2. Self-folding systems with differentially swelling hydrogel actuators**

Curling and curving of hydrogels can be accomplished in the presence of a bilayer system, where the swelling characteristics of each hydrogel layer vary, leading to preferential curling along a particular side.[33] Guan et al highlight a method to create a differentially swelling hydrogel bilayer using solvent casting and photocuring. PDMS molds were created using soft lithography. These microstrips of chitosan were released from the PDMS molds using a sticky substrate for the microstrips to adhere to and come off the mold. The sticky substrate was made of PVA on a glass slip. This also acted as a sacrificial layer so upon addition of water, the PVA layer dissolved to release the microstrips from the glass plate and the DI water also allowed the water to swell. Adding an extra layer of PEGMA-co-PEGDMA to this chitosan layer followed by the same method of release and lift off led to the formation of curled structures that curled due to differential rates of swelling to the two layers in the hydrogel bilayer.[34] It has been suggested that the PEGMA molecules tended to form a semi IPN with the chitosan layer, and led to a strong bonding between the two layers. The PEGMA-co-PEGDMA layer swelled more than the chitosan layer, which caused the structures to curl away from the PEGMA layer. Gracias summarizes articles that report this phenomenon.[35] Figure 1 relays the various kinds of bilayers that could exist to allow a system to foldout of plane.

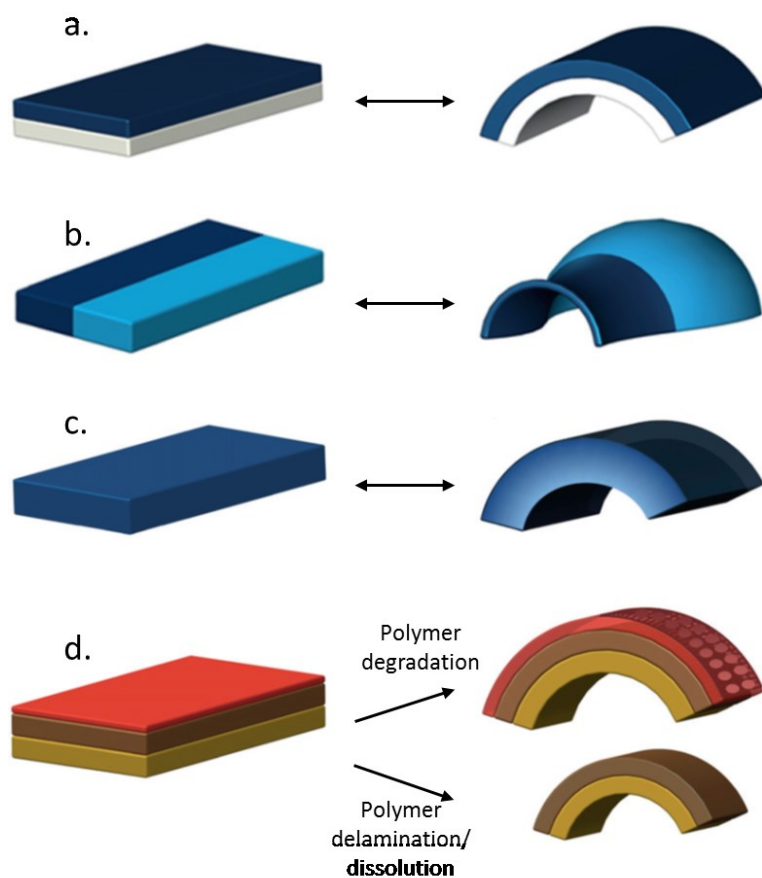


Figure 1 - A schematic of the ways a polymer system can bend out of plane. a.) Bilayer of polymers that undergo differential swelling, b.) Laterally arranged polymers that undergo differential swelling, c.) Polymer with a crosslinking gradient along its thickness, d.) Incorporation of a trigger layer that can be eliminated to cause bending of the strained bilayer underneath. Reprinted with permission from Ref. [36] © 2013, Current Opinion in Chemical Engineering.

Erb et al developed a composite material consisting of aligned stiffer regions oriented a certain way in a polymer matrix, which tended to drive the way the polymer responded to the applied stimulus. This is based on Nature's strategies which drive pine cones to respond to humidity or seed dispersal mechanisms that are put into play in the presence of moisture.[37] The shape of a material also plays a role in deciding how it might fold. Shape programming in a stimuli responsive material brought about predictive folding upon changing the stimulus, as reported by Stoychev et al.[38]

Wu et al mimicked plant tissue by programming bands of differential stiffness into a homogenous flexible sheet. This brought about various swelling forms like helices or simple bending of this rectangular composite, based on the angle of the bands in the rectangle.[39] Ionov reviews the hydrogel actuators; actuation can be brought by adding a stimulus that the hydrogels respond to, programming them by fixing their shape or by the incorporation of stiffer components into the matrix which causes a structural inhomogeneity. The review also touches upon the limitations of hydrogel actuator systems.[40] Randhawa et al describe a new class of systems called MCMS (microchemomechanical systems) that respond to stimuli other than electricity, and this spurs actuations in their structures.[41]

Hawkes et al wrote about creating origami using a flat sheet of geometrically arranged shapes which could align in multiple orientations. These are programmable materials which could change shape or stiffness depending on the environment they are placed in.[42] Their paper highlighted how a certain arrangement of rigid parts in a flat orientation could fold into 3-D origami if it were preprogrammed to do so. This finds application in user friendly which could be morphed and remorphed as per the user's requirement.

Stoychev et al created a stimuli responsive actuator system that responds in a hierarchical manner to create 3-D folding shapes with hinges that are sharp due to sequential folding of the polymers along the sides which triggers a folding of the shape out of plane.[43]

### **1.3. Nature undergoes bidirectional folding**

Certain responses in Nature that depend not on cellular activity, but on external stimuli are attractive inspirations for designs in engineering. Upon understanding the mechanics of a natural phenomenon, biomimicry in engineering can employ stimuli responsive materials for a real world application of this.[44] Examples of biomimicry in this aspect exist in avenues like drug delivery, structural construction, electronics or catalysis.[20], [45] The natural systems that we investigate perform passive movement that do not involve cellular metabolism to initiate the movements, but are solely driven by physical changes in the macro and microstructure of the system. Janet Braam highlights these nastic movements in plants, which occur in a few fractions of a second.[46]

The different mechanisms of organ movement have been highlighted by Burgert and Fratzl. [47] They cover passive movements of plant systems that deal with the influx or efflux of water from the cellulose fibrils in the microstructure of the plants, which leads to actuation of the plant structure. The various mechanisms that can trigger actuation are due to variation in turgor pressure as in the case of Venus flytraps and mimosa plants[48], [49], cohesion forces, cell growth, and cell wall swelling and shrinking as in the case of ice plant or pine seed dispersal processes.[50], [51] They go on to touch upon the requirements of an actuating composite that functions on the principles of cell wall swelling and shrinking. Ionov highlights the reversible plant movements that inspired reversibly actuating hydrogel systems with differential strain being the factor that drives actuation[52]

Fratzl and Barth also cover this in their review on the biomaterials that are involved in actuation and mechanosensing. They touch upon Venus flytraps being the fast actuating plants while slower actuating plants exist too, along with other types of hairs for mechanosensing.[53]

Harrington et al studied the structural changes that an ice plant seed undergoes in the presence of an external stimulus.[50] The protective casing around the seed consists of a bilayer of opposing tissue orientations which opens only in the presence of liquid water, thus ensuring that the seeds will be dispersed in the appropriate conditions to allow germination. The unfolding of the plant follows a “flexing and packing mechanism” in presence of water, within minutes to over 150°. The inner layer of the bilayer has a tendency to absorb more water compared to the outer layer which causes this bidirectionality during the unfolding. Mahadevan and Rica discuss the mechanics behind the Miura Ori pattern on the hornbeam leaf that arises due to the biaxial compression of a thin, stiff layer on a softer substrate.[54]

Bidirectional folding in the case of the Venus flytrap is due to a snap-buckling instability as mentioned by Forterre et al.[55] The leaf is curved outward when open and curved inward when closed. For a surface curved along two axes, when there is a bending component along one axis, there is inadvertently a stretching component along the other axis. If this relation is strong, there might be a large change in bending needed to induce a snap change in stretching and vice versa, which is the case of the Venus flytrap and could potentially be the case in our system. Biomimicry has been employed by a number of scientists to create this fast action based on mechanical instabilities with changes in stimulus and this has led to interesting inventions.

Breger et al created a thermoresponsive magnetically controlled system to move cargo.[28] Holmes and Crosby created a surface that undergoes a snap-response upon the introduction of an organic solvent, which caused the microstructures on the surface to snap from a concave orientation to convex structure.[56] Sidorenko et al created a reversibly



actuated stimuli responsive composite of nanofibers supported on a hydrogel substrate that bend based on the presence of an environmental humidity.[57]

#### **1.4. Stimuli responsive materials**

Beginning in the 1960s, a recognition of the need to shift from conventional drug delivery systems to more specialized mechanisms that targeted the area of interest using local physiological triggers to release the therapeutic cargo in a controlled fashion.[58] Polymer drug delivery systems were rigid at the site of delivery and there was also a need to investigate more flexible options of drug delivery which would release the drug in a controlled fashion spread out over longer time intervals. Hydrophilic polymers which form an intricate mesh to trap water molecules and swell, thus using osmotic pressure to release the therapeutic cargo began to be investigated. There was a drive to create biocompatible, biodegradable hydrogels whose swelling patterns could be triggered by the changes in local environment in the form of temperature, pH or in the presence of certain species like proteins or metal ions.[59]–[61] There isn't a very dramatic change in temperature in the human body but temperature responsive hydrogels gained importance due to the change in properties when introduced into the warmer body from an external colder environment. There exist very good reviews about stimuli responsive materials in literature.[35], [41] This section in the thesis reviews the hydrogel systems that respond to stimuli, thermoresponsive hydrogels being the most focused on. PNIPAAm is the model thermoresponsive hydrogel system which has been studied extensively for use in drug delivery and in the creation of stiffer scaffold materials for surgical applications. The mechanism by which this responds is due to its low LCST where it transitions from a hydrophilic to hydrophobic state as temperature increases above 32°C. Stimuli responsive hydrogels allow for some varied applications in broad fields of study like surface coatings, cell culture, biomedical actuators etc.[62]–[64]

pNIPAM is an interesting phase transitioning hydrogel that can undergo a dramatic change in volume based on an external stimulus like temperature.[65], [66] It expresses a lower critical solution temperature (LCST). Increasing the temperature of the hydrogel above the LCST causes the pNIPAM gel to collapse due to increased hydrophobic interactions.

Work was performed by Tanaka et al to understand how phase transitions could result from ionization within the gel matrix or changes in pH within the gel.[67] The presence of acrylamide groups in the chemical structure of the hydrogel can bring about the possibility of conversion to acrylic acid groups and hence, scope for phase transition. This is due to the osmotic pressure of hydronium ions created from the ionizable groups, hence even varying the pH of the gel could bring about a phase transition. Of importance to this thesis, is the LCST of the pNIPAM hydrogel on a macro scale. The quantitative explanation for the collapse of the hydrogel is explained in the Flory Rehner Theory.[68]

The theory in the chemistry of collapse of pNIPAM beyond LCST and how to measure it and relate it to the environment of the hydrogel, has been looked into by a number of research groups. Wongsuwarn et al describe the structural changes that the pNIPAM mesh undergoes beyond the LCST.[69] At room temperature, water molecules interact through hydrogen bonding with the amide groups of pNIPAM. The hydrophobic groups are extended out in this random coil structure, in a clathrate formation, of lowest free energy. As the temperature increases, entropy of the clathrate structure increases. If this term increases above the LCST, the free energy associated with hydrogen bonding becomes positive, and no longer the lowest energy state, leading to an instability in the system which causes the coils to collapse. The new globular structure is more compact and allows for the hydrophobic regions to be better shielded from the water which is now a bad solvent.

A very detailed review on this topic of pNIPAM swelling chemistry was presented by Schild et al.[70] They made a number of points, such as, the LCST, at which the collapse of the pNIPAM structure occurs, depends on the microstructure of the polymer. pNIPAM can be prepared in organic or aqueous media, and can be polymerized by radical polymerization or ionic polymerization due to the transfer of hydrogen ions. Crosslinked gels use recipes that involve N,N'-Methylenebis(acrylamide) or BIS which is favorable due to its structural similarity to NIPAM. Increasing the number of ionic groups in the pNIPAM gel structure leads to the transition from hydrophilic to hydrophobic becoming sharper. pNIPAM contains components that tend to interact differently with water molecules. Some show like interactions such as specific orientations for hydrogen bonds, and others show unlike interactions, like hydrophobic effects which lead to clathrate like structures of water around the collapsed hydrophobic mesh of the hydrogel above the LCST. Above the LCST, the entropy of mixing decrease dominates the exothermic enthalpy of hydrogen bonding between polymer and water molecules. Once the  $\Delta G$  becomes positive, precipitation happens above the LCST. The debate lies in which of the two causes the collapse - hydrophobic effects or hydrogen bonding. A number of publications talk about how hydrogen bonding could be the main reason for the LCST, because only certain orientations in the polymer allow for hydrogen bonding. There are four energy terms associated with a polymer with LCST. If the polymer is ionically charged, there exist osmotic effects, and the other energies are those associated with mixing, elasticity and maybe hydrogen interactions.

Mao et al devised a system to demonstrate a setup to capture collapse data of the hydrogel in the presence of a temperature gradient, independent of time.[71] Zhang et al studied the effect of various ions in solution on the LCST of the pNIPAM polymer structure.

The properties of pNIPAM can be better tuned and made more predictable upon adding co-monomer units into the NIPAM stock solution, and hence the resulting hydrogels are now thermo and pH responsive.[72] Other modifications in swelling nature and increasing the thermal sensitivity of the hydrogel can be brought about by creating semi-IPN networks with higher swelling capabilities.[73]–[75] Work by the Gracias lab uses photolithography to create shapes of these polymers to create hinge materials for actuators. They use the swelling properties of the stimuli responsive hydrogels to create folding bilayers which are reversibly triggered by different stimuli.[76]

## CHAPTER 2. REVERSIBLE BIDIRECTIONAL FOLDING OF A HYDROGEL SYSTEM

### 2.1. Introduction

When a Venus flytrap snaps, the orientation of its leaves undergo a transition from being concave to convex, as viewed from the outside. This was a milestone observation and insight into how snap instabilities in a structure can contribute to movements in the plant kingdom that last over a fraction of a second.[56] This subtle change in shape leads to a more robust mechanism of trapping prey within its leaf structure. This has been highlighted in Figures 2 and 3 below. This action is osmotically driven and dominated by mechanical alignment. Other osmotically driven plant movements are in the case of stomata.[47], [77]



Figure 2 - The actions involved in a Venus Flytrap snapping shut to catch its prey. Image obtained from <http://www.naturalhistorymag.com/biomechanics/112001/snap>

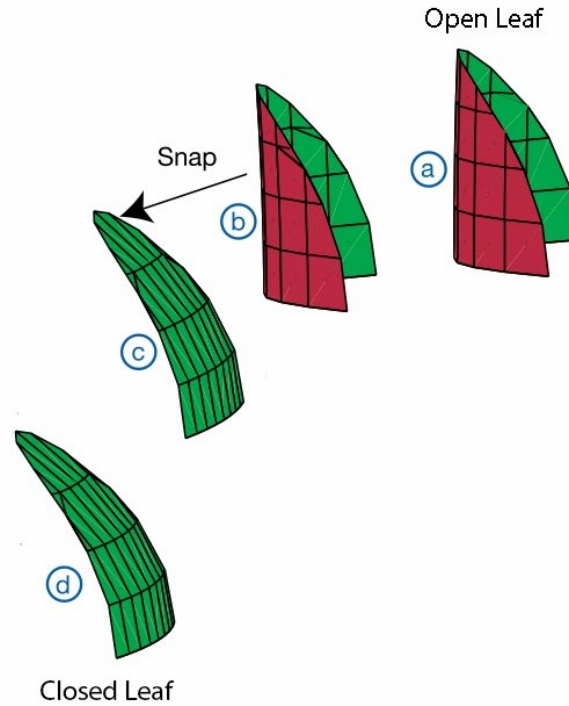


**Figure 3 - The changes in the orientation of a Venus Flytrap leaf in action, when closing on prey. The orientation of the leaf changes from concave when open to convex when closed. Reprinted with permission from Ref. [49] © 2005, Nature.**

Other fast acting movements in Nature can be observed due to the quick variation of turgor pressure in response to atmospheric moisture, as in the case of the ice seed capsule, where the unfolding of the leaf occurs only when wet, leading the leaf to swell and open, due to the programmed alignment of the swelling cellulose layer in the leaves, which constrains the swelling.[50] This is the plant's way to ensure that the seeds can be dispersed in an environment that contains water, essential for the growth of the new plant. This leads to the discussion of how Nature “programs” stiffer components into the hydrogel matrix of a leaf or stem, to enable certain movements and facilitate a certain kind of growth of the plant tissue.[78] Wheat awns are hygroscopically controlled to coil or uncoil, and this variation in alignment propels the seeds to the ground, much like a programmed motor. This motion is

completely driven by the moisture in the environment and water absorption by dead plant tissue, and not by chemical changes in the live plant tissue.[79] A similar environmental moisture driven actuation can be observed in the case of pine cones, where the scales open in the presence of low moisture or drier conditions and close up in the presence of wetter conditions.[51]

The instance of the ice seed capsule brings to light, how geometric alignments and a hierarchical structure of stiffer segments arranged in a flexible, reversibly swellable hydrogel allow for folding like those observed in origami, which contains instances of effective packing and flexing mechanisms, as seen in miura ori.[80] An example of a miura ori pattern can be seen below (Figure 4, Figure 5).

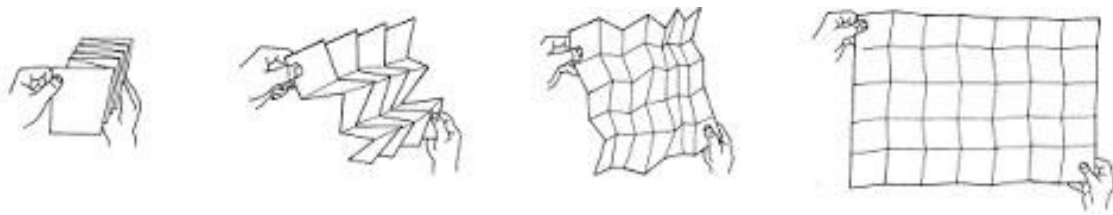


Figure 4 - Miura ori pattern can be created using origami, contains interrelated folds that allow the entire sheet to be folded into a compact form by the application of a unidirectional force. Image obtained from <http://www.origami-resource-center.com/origami-science.html>

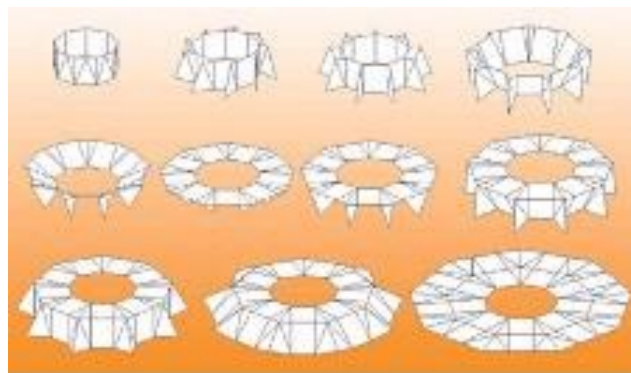


Figure 5 - Miura ori employed in the design of a telescopic lens, that can be packed onto a satellite and unfolded in space, at the time of need, once the satellite has safely been incorporated into orbit. Image obtained from <http://www.origami-resource-center.com/origami-science.html#eyeglass>

Miura ori is a popular origami pattern wherein a number of folds incorporated into a flat sheet of paper could allow the use of two directions to fold it into a more compact form.[81] Nature seems to naturally express this miura ori pattern, as shown by Mahadevan and Rica.[54] Named after the creator, Koryo Miura, this pattern involves a series of geometrically aligned folds that rely on each other when the plane is folding and unfolding, such that the whole plane can be folded or unfolded at the same time. The hornbeam leaf has been naturally endowed with this pattern, which aids the leaf to unfold during stages of its development. This pattern is proving as useful inspiration in designing prototypes in various fields like solar power and biomedical applications.[80], [82]–[85] Tolley et al used shape memory composites, patterned in a particular manner, which were activated by heat to self-fold into a miura ori pattern.[86]

Research involving “programming” a responsive material with stiffer components has been conducted by multiple groups thus far. Numerous academics have reviewed this topic of programmable materials.[87] Work by Hawkes et al uses triangular tiles in a sequentially arranged manner to create a sheet that folds into various 3-D shapes like a boat or airplane by programmed origami of the hinge material in response to an electric stimulus.[42] Ionov reviews the various stimuli responsive hydrogel actuated systems, and describes that discontinuous actuation can be brought about in the presence of a stimulus, by applying an inhomogeneous gradient in the stimulus, or by incorporating a layer of a hydrophobic, non-swelling polymer.[14], [52] Liu et al show the effect of infrared light on a prestressed polystyrene sheet, with black lines printed on it, which cause the parts of the sheet at the lines to heat up and attain the glass transition temperature before the rest of the sheet, and hence,



act as a hinge material at which the 2D shape folds into a three dimensional structure.[88] This has been highlighted in Figure 6.

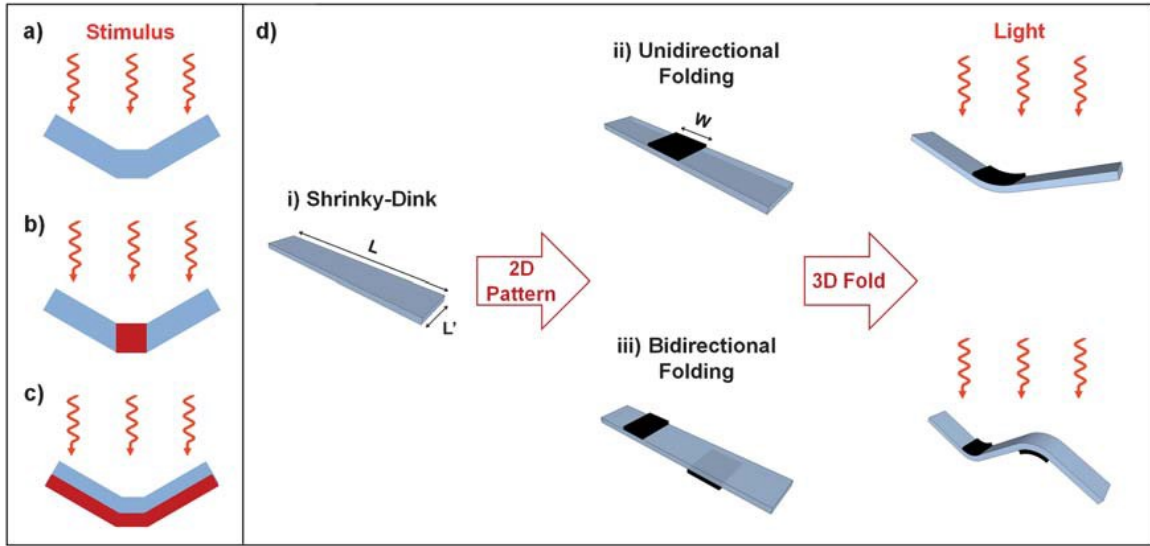


**Figure 6 - Folding of a prestressed polystyrene sheet at the hinges, which are black lines printed on the sheet, which attain glass transition temperature before the unmarked regions of the sheet.**  
Reprinted with permission from Ref. [88] © 2012, Soft Matter

Turcaud et al studied how geometrically symmetric breaks in the cross section of a rod and incorporation of a differently swelling material into those breaks can lead to various conformations of the rod like bending or twisting.[89] Analytical solutions have been calculated for the case of a plate of lenticular thickness subjected to a temperature gradient. Steeper gradients tended to show a preference for plate curvature along the longer side.[90]

Lee et al created a PEGDMA structure that undergoes a snap instability, like a Venus flytrap. The system consists of a doubly curved stiffer hydrogel with thin channels to allow for water to seep through by capillarity, but also begin to soak into the polymer, causing a snap instability.[48] Another Venus flytrap mimicking system is that of the snapping surfaces, which are on the edge of a snap instability, sensitive to a very small mechanical force or change of

solvent, which is enough to cause the surface swell and snap.[56] Smela et al have shown how different sides of a rectangular bilayer are the dominant sides along which folding occurs, for thin bilayers, based on different methods of fabrication.[91] Li et al demonstrated how thin films with mismatched strain tend to undergo a rolling deformation, the direction of which depends upon the fabrication history, the method of liftoff or etching to allow for strain reduction and dimensions of the rectangle.[92]

Also of interest, are shapes that have laterally varying swelling capabilities that deform into various 3-D structures and form complex features that express a Gaussian curvature. Sharon and Efrati created differentially crosslinked non-Euclidean surfaces whose stable structure was a 3-D form exhibiting a Gaussian curvature.

Kim et al created regions of different crosslinking densities on a sheet of a hydrogel using photolithography. This resulting shape would need to curve in a 3D configuration to minimize the in plane stresses. Differentially exposed regions of the gel swelled at different rates[93] Schenning and coworkers came up with a method to create liquid crystalline polymers that were held together by hydrogen bonds, which were activated and deactivated by humidity variations.[94] Xu et al created a bilayer which contained two layers of varying concentrations of pNIPAM in a  $\text{TiO}_2$  crosslinked nanocomposite hydrogel, with the pNIPAM increasing the mechanical strength and swelling ability of the hydrogel. Two different layers of this hydrogel formed a differentially swelling bilayer, which tended to curl one way in the presence of 20% NaCl solution, and uncurled, flattened out and curled the other way in the presence of pure water. They stated this was the bilayer undergoing bidirectional folding.[95]

This thesis considers bidirectional folding to be different from the above definition. Bidirectional folding, henceforth, is going to be referred to as one that undergoes folding along

the short side facing in the upward direction, and then undergoing a flip in curvature to be curved along the long side and facing the downward direction.

Along these lines, an interesting system would be one which consists of stiffer components, geometrically arranged on a reversibly responsive swelling hydrogel, which influence the folding of the hydrogel layer to a large extent by restricting its ability to fold. The system described in this chapter exhibited a bistability, which caused it to assume two varying forms across a temperature gradient. The polymer system comprised of a swelling hydrogel, poly (N-isopropylacrylamide) or pNIPAM, with grids of SU-8, a non-swelling polymer photoresist. This system was created using photolithography. pNIPAM is a thermoresponsive hydrogel with a lower critical solution temperature (LCST) of around 31°C.[70] The hydrogel system folded one way at room temperature (25°C) and then it snapped the other way beyond the LCST. This can be better pictured as in the Figure 7.

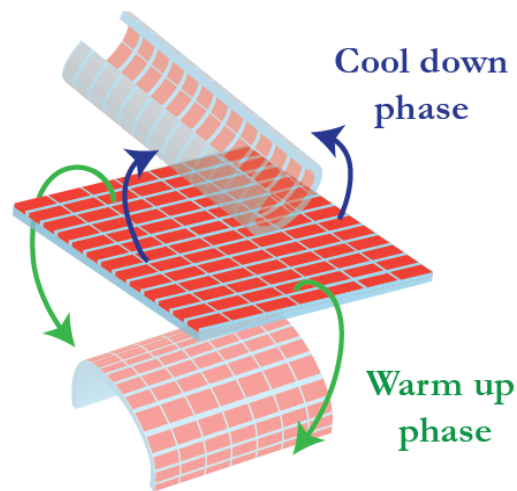


**Figure 7 – A schematic of the bidirectional folding capability of the thermoresponsive hydrogel system**

## 2.2. Fabrication and experiments

The system comprised of a rectangular sheet of the flexible, thermoresponsive pNIPAM, with stiffer non swelling grids of SU-8 embedded in the sheet. The top view of the system with dimensions has been shown below. (Figure 8)

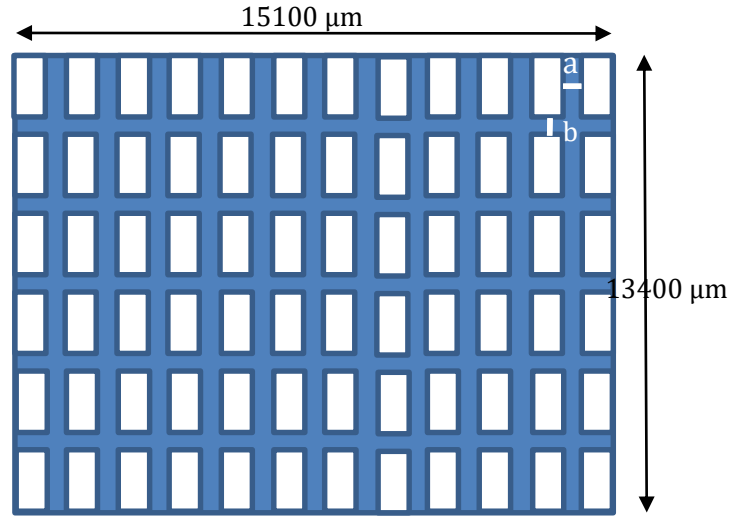


**Figure 8 - Top view of the bidirectional folding hydrogel system design, with dimensions. The blue region represents the hydrogel sheet while the white rectangles are the grids of non-swelling SU-8 photoresist. The spacing between the grids varies as:  $a = 500 \mu\text{m}$ ,  $b = 400 \mu\text{m}$ .**

The masks for this system were created using AutoCAD. The aspect ratio was 2.375:1 for the SU-8 grids, the length being 1900  $\mu\text{m}$  and width being 800  $\mu\text{m}$ . A portion of the mask has been shown below, indicating one shape. At a time, nine shapes were fabricated. The fabrication schematic has been shown in Figure 10.

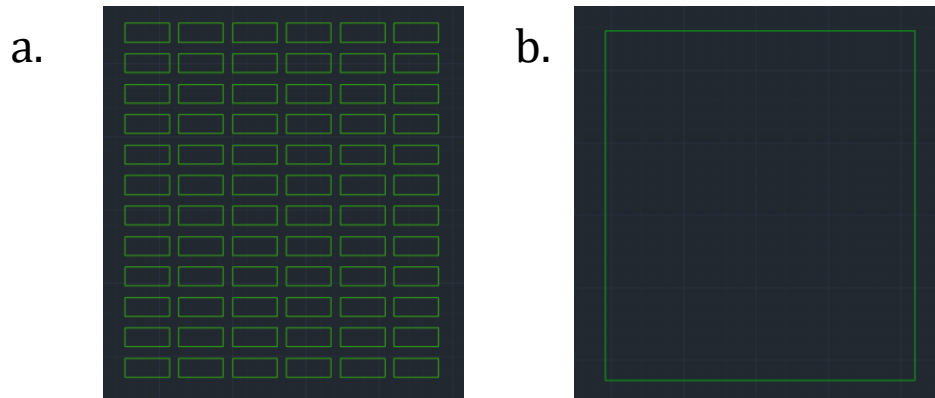


Figure 9 - Negative masks for the hydrogel system. a. SU-8 mask for the stiff non swelling grids, b. rectangular shape for the pNIPAM layer of the hydrogel system.

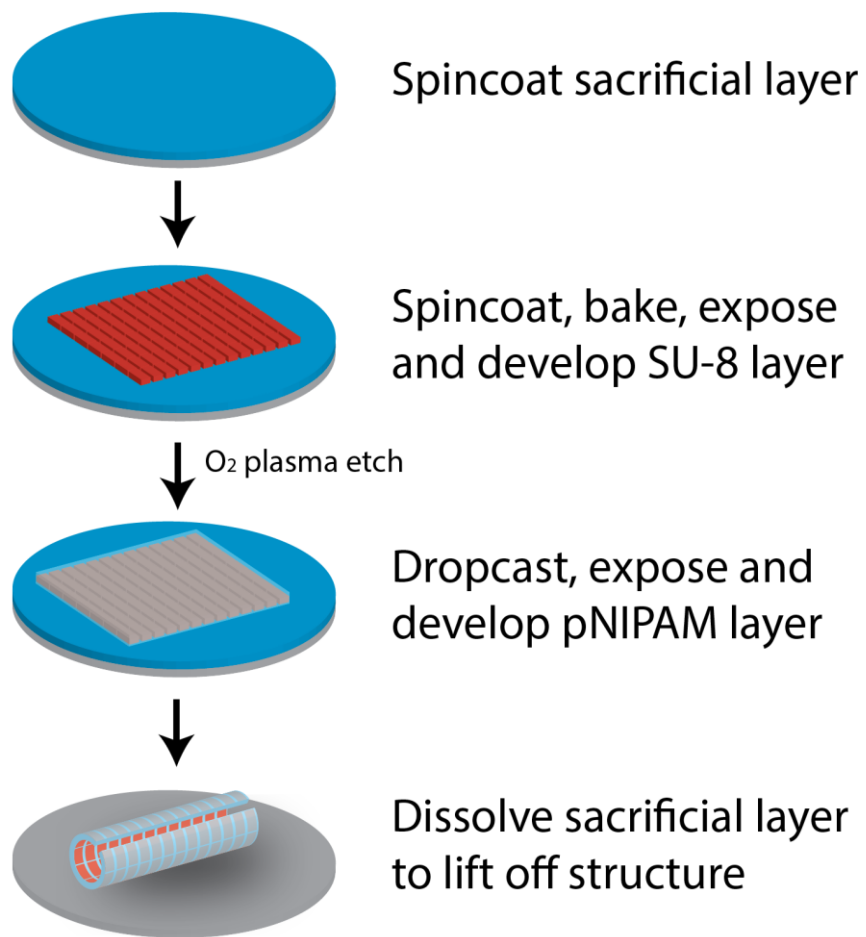


Figure 10 - Microfabrication schematic of the hydrogel and grid system.

The fabrication began with preparing the stock solutions for the two layers and a sacrificial layer. The sacrificial layer was PVA (polyvinyl alcohol, Sigma Aldrich, 9000 Da molecular weight, 80% hydrolyzed), and the stock solution was a 1:10 ratio by weight of PVA in DI water, stirred overnight and set aside. The next stock solution to be prepared was that of pNIPAM, which followed the protocol stated by Bassik et al.[76] Briefly, a mixture of NIPAM monomer, pNIPAM, BIS-acrylamide, 1-butanol, acrylic acid and Irgacure© were stirred overnight, and covered and stored until further use.

The fabrication was performed in the clean room, where a silicon wafer was cleaned with acetone, IPA and dried with a stream of nitrogen. This was then placed in a spincoater, and a small amount of PVA solution was aliquoted on it. The wafer was then spun at 2000 rpm for one minute, and transferred to a hot plate to bake for five minutes. Upon returning the wafer to room temperature, it was placed back on the spincoater, and this time a small amount of SU-8 2025 photoresist (Microchem) was aliquoted onto it. Care was taken to not allow air bubbles to be present in the SU-8 aliquot, these were removed by another transfer pipette. The SU-8 layer was spun at 3000 rpm for one minute following a ramp protocol. The wet layer of SU-8 was baked, to allow the volatile solvents to evaporate and to allow the layer to harden. The wafer was thus transferred onto a hot plate to bake for two minutes at 65°C, five minutes at 95°C and two minutes at 65°C, until the SU-8 layer hardened. It was then allowed to come to room temperature. This was then exposed to 500 mJ/cm<sup>2</sup> of UV light, in a mask aligner (Quintel) through the mask. The post exposure bake consisted of baking at 65°C for one minutes, 95°C for 5 minutes and 65°C for one minute. Upon cooling back to room temperature, the wafer was placed in SU-8 developer for 1 to 1.5 minutes until the unexposed regions of the wafer were completely dissolved, rinsed with acetone and IPA, and then only the crosslinked grid features were visible. The next step was to oxygen plasma clean

the surface of the SU-8 layer, and the wafer was placed into the oxygen plasma etch for 480 seconds at 30 RF. Immediately after this step, 1 ml of pNIPAM stock solution was drop casted onto the surface of the wafer and levelled. This wafer was then exposed to 60 mJ/cm<sup>2</sup> of UV light, through a mask separated from the wafer using spacers, in non-contact lithography. The two layers were allowed a period of four hours to establish good bonding between the two layers, following which, DI water was added to the Petri dish containing the samples to dissolve the sacrificial layers, and lift off the shapes and let the pNIPAM hydrogel layer swell.

The experimental setup involved one of the shapes being placed under water at room temperature in a glass petri dish. This petri dish was placed on a hotplate, set to 95°C to allow the water temperature to increase, and hence to study the response of the shape to this temperature increase. The response was captured using a camera, positioned directly above the hotplate, to capture a series of time lapses through the DIY PhotoBits software. The phase when the sample was placed on the hotplate was called the warmup phase, and at the end of the warmup phase, the final state was noted. During the course of the warmup phase, the temperature was noted as a function of time, to obtain the rate of temperature increase. The transition temperature of the hydrogel was observed to be approximately 30°C, and by 40°C, the final state of the shape was established. Hence, the warmup phase was stopped at 40°C.

The petri dish containing the warm water and the transitioned sample was then allowed to cool down under ambient conditions, and the temperature was still recorded as a function of time, and time lapses were still taken of the shapes. As the system hit about 30°C, it began to unfold and transitioned back to its original state. The cooldown cycle was stopped when the shape was back at room temperature. One cycle comprised of a warmup and cooldown

phase. The notation followed stated that during the first cycle of cycle 1, the warmup phase was called “w1” and the cooldown phase was called “c1”.

These shapes were stored at room temperature under water for up to three days, after which the hydrogel’s temperature response began to deteriorate slowly, and the transition temperature of the hydrogel increased to above 31°C.

### **2.3. Results and Discussions**

The lifted off sheets tended to curl as they swelled, with the pNIPAM layer swelling on the outer side, and the SU-8 grids being on the inner side of the hollow cylinder. This form has been shown more vividly in the last step of the fabrication schematic in Figure 10. Most of the shapes tended to curl along the short side. Figure 11 is a time lapse capturing the liftoff curling of two shapes, with beads on the pNIPAM layer, which roll off, indicating that the pNIPAM layer was on the outside as the shape curls, along the short side. Henceforth, the notation of pNIPAM layer on the outside where curling is towards the SU-8 grids, away from the pNIPAM layer, is concave. Curling towards the pNIPAM layer, away from SU-8 is referred to as convex. When the breadth of the rectangle is curled, it is said to be curled along the short side and when the length is curled, it is referred to as being curled along the long side. An instance of the liftoff to show the shape being concave along short side is shown below.



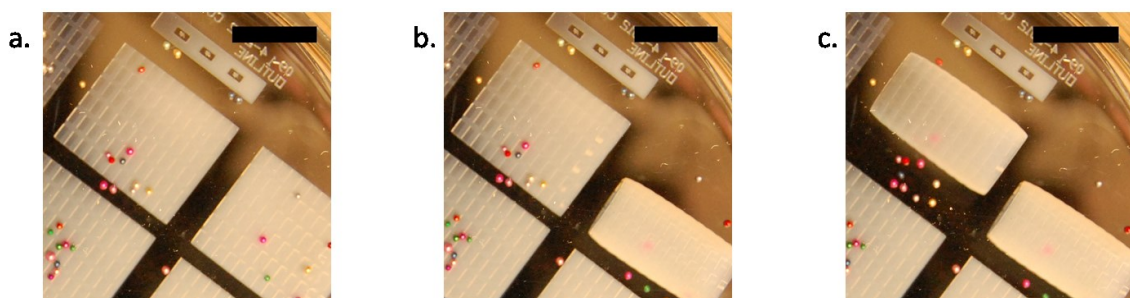


**Figure 11 - Liftoff of shapes from the wafer, the last step of the fabrication process to show how the shapes naturally curl concave along the short side. The beads roll off the surface, proving this.**

Scale bars: 1 cm

Each shape started out as being curled concave along the short side. When it underwent the warmup phase, it was observed to begin uncurling at 27°C until it became nearly flat at 30°C, following which it became convex curled along the long side. This was an indication of the pNIPAM thermoresponsive nature where it began to collapse as the temperature increased, and underwent a sharp transition around 30°C where the hydrophobic interactions in the hydrogel became more dominant and this led the water molecules to diffuse out of the gel matrix, leading to its collapse. When placed off the hotplate to undergo cooling under ambient conditions, the pNIPAM began to absorb water, and underwent a sharp swelling transition about 30°C to become hydrophilic again. Figure 12 gives a better visual aid into this bidirectional folding behavior.

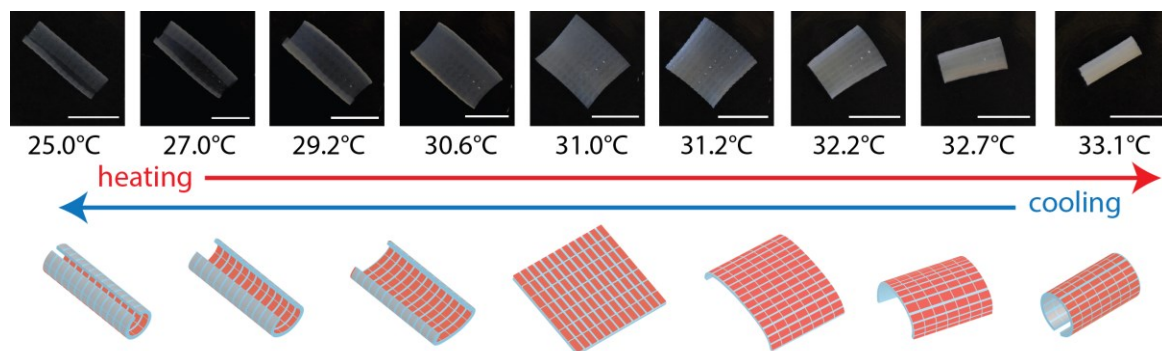


**Figure 12 - Bidirectional folding schematic with images from experimentation**

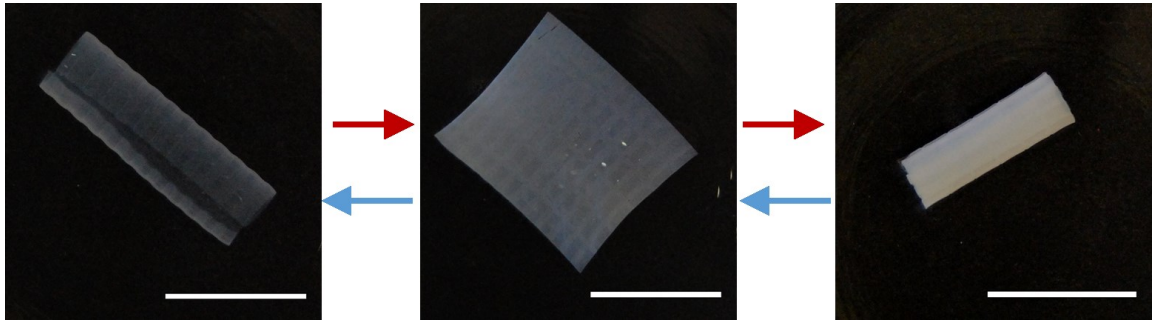


**Figure 13 - Images from the bidirectional folding experiments, the leftmost image is the beginning of a warmup phase, the image in the middle shows the flat state in transition, the image on the right shows the shape at the end of the warmup phase. The red arrows indicate the warmup phase, the blue arrows indicate the cooldown phase. Scale bars: 1 cm.**

The results of the warmup and cooldown phases were tabulated, for up to three cycles of the shapes, which means that the bidirectional folding was reversible for up to three cycles of warmup and cooldown. The table below shows the results for various cycles of the shapes in the 2.4:1 aspect ratio system.

**Table 1 - Results of bidirectional folding for shapes with aspect ratio 2.4:1 (3 viable samples)**

	temp rate (°C/min)	start	end
w1	1.89	100% curled convex-short side	100% curled concave long side
c1	0.5	100% curled concave long side	100% curled convex short side
w2	1.29	100% curled convex short side	100% curled concave long side
c2	0.44	100% curled concave long side	100% curled convex short side
w3	2.79	100% curled convex short side	100% curled concave long side

c3	0.42	100% curled concave long side	100% curled convex short side
w4	2.38	100% curled convex short side	100% curled concave long side

These results were compared to those of systems where the aspect ratio of the SU-8 grids varied as 1:1 and 1:2.375. The spacing between the grids was different from the original system, because care was taken to maintain the outer dimensions of the overall shape, where the length is 15100  $\mu\text{m}$  and breadth is 13400  $\mu\text{m}$ . The masks for these are shown below.

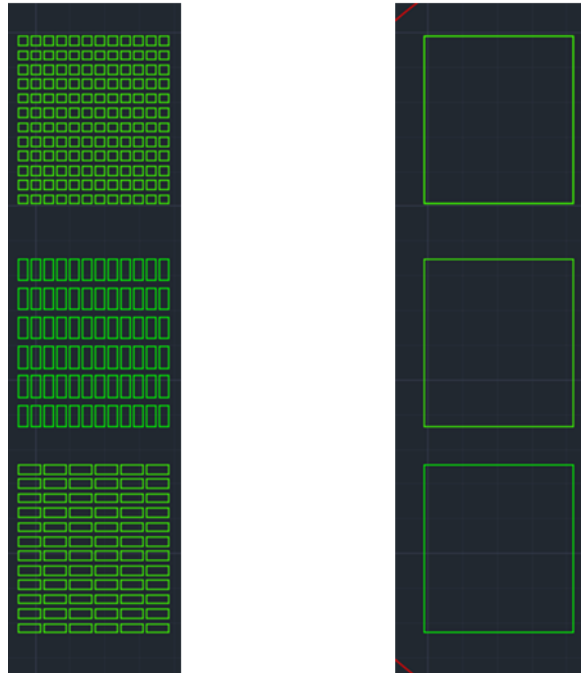


**Figure 14 – (Left) Mask of the systems to be studied for bidirectional folding dependence on aspect ratio. Of the SU-8 mask on the left, the bottom three shapes indicate the original system with SU-8 grid aspect ratio = 2.375:1. The square grids indicate 1:1 aspect ratio, of side length = 800  $\mu\text{m}$  and the remaining grids are of aspect ratio 1:2.375. (Right) pNIPAM masks corresponding to the SU-8 masks.**

The results for these shapes were tabulated below.

**Table 2 - Results of the bidirectional folding experiment for the shapes with aspect ratio 1:1 (4 viable samples).**

	temp rate (°C /min)	start	end
w1	3.56	100% are convex short	100% are concave long
c1	0.43	100% are concave long	100% are convex short
w2	2.5	100% are convex short	50% are concave long
c2	0.55	50% are concave long	50% are convex short
w3	2.3	50% are convex short	75% are concave short
c3	0.9	75% are concave short	75% are convex long
w4	2.06	75% are convex long	50% are concave short
c4	0.55	50% are concave short	50% are convex long
w5	2.2	50% are convex long	50% are concave short

**Table 3 - Bidirectional folding experiment results for samples with aspect ratio 1: 2.4 (5 viable samples).**

	temp rate (°C/min)	start	end
w1	3.15	100% curled concave long side	100% curled concave long side
c1	0.51	100% curled concave long side	100% curled concave long side
w2	2.98	100% curled concave long side	100% curled concave long side
c2	0.53	100% curled concave long side	100% curled concave long side
w3	3.08	100% curled concave long side	100% curled concave long side
c3	0.4	100% curled concave long side	100% curled concave long side
w4	0.13	100% curled concave long side	100% curled concave long side

Additional experiments were carried out to confirm the onset of bidirectional folding. The shapes comprised of varying numbers of rows and columns, the mask of which has been shown below. The shapes were annotated with number of rows, and columns of the SU-8 grids, in a matrix form, assuming each grid is horizontal with aspect ratio 2.375:1, as was in the original case. Each row contains six grids, and each column contains 12 grids.

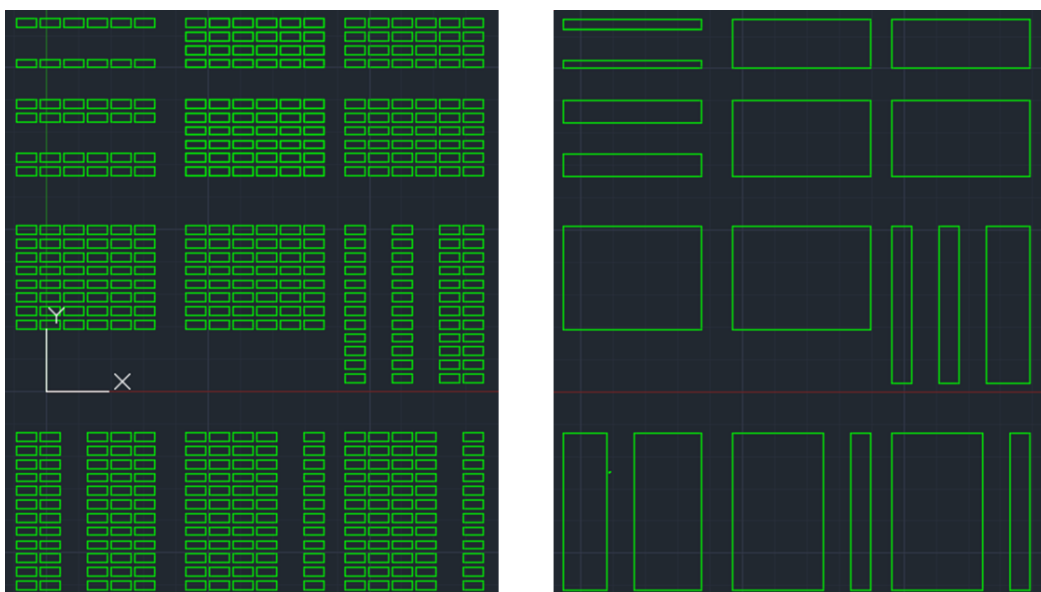


Figure 15 – (left) investigating the onset of bidirectional folding by varying the number of rows and columns of SU-8 grids. (Right) The pNIPAM masks corresponding to the SU-8 masks.

The results of these investigations have been tabulated below.

Table 4 - Effect of varying the no. of rows and columns, on bidirectional folding

SU-8 shape [rows, columns]	pNIPAM sheet length ( $\mu\text{m}$ )	pNIPAM sheet width ( $\mu\text{m}$ )	Expresses bidirectional folding (Y/N)
[1,6]	13400	800	N
[2,6]	13400	2100	N
[4,6]	13400	4700	Y
[6,6]	13400	7300	Y
[8,6]	13400	9900	Y

[12,1]	15100	1900	N
[12,2]	15100	4200	N
[12,3]	15100	6500	Y
[12,4]	15100	8800	Y

Another study was performed to analyze the grid system with aspect ratio 1:1, to keep the pNIPAM sheet dimensions constant, but to vary the size of the grids, and hence their spacing. The purpose of this was to see whether bidirectional folding was expressed in the system with square grids, and at what point. The masks for these have been shown below and results have been tabulated (Table 5). The squares vary from 200  $\mu\text{m}$  to 800  $\mu\text{m}$  and there were 12 rows and columns in each shape.

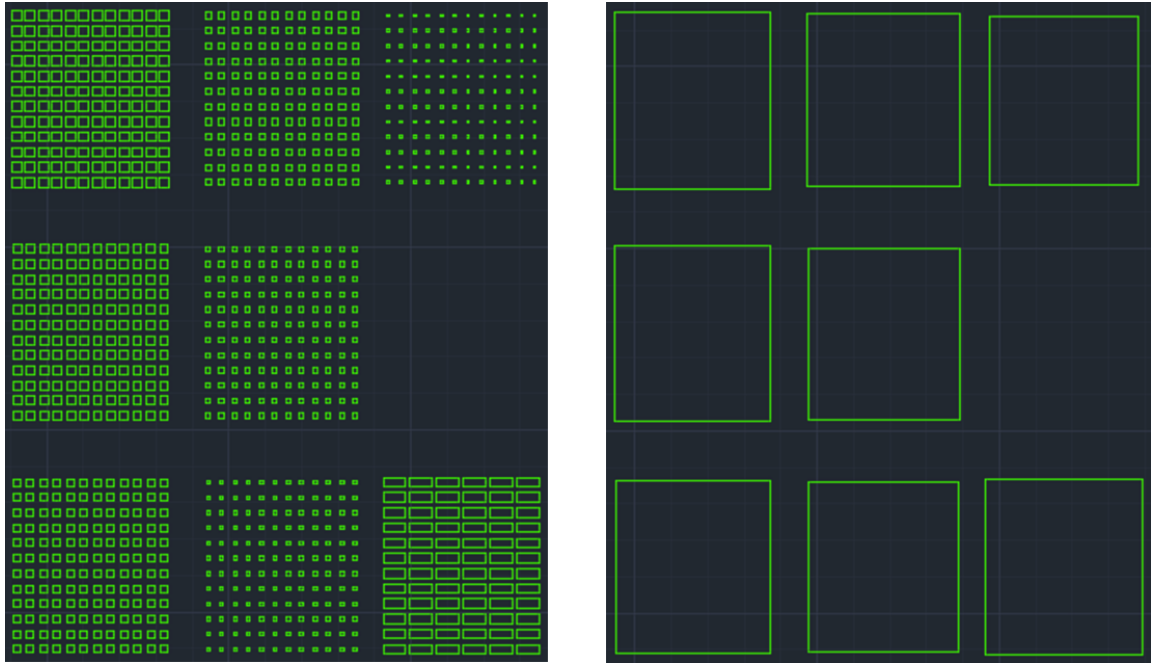


Figure 16 - (left) SU-8 masks to study the dependence of bidirectional folding on square grid dimensions. (Right) the pNIPAM masks corresponding to the SU-8 masks

**Table 5 - The dependence of bidirectional folding on the size of the square grids**

SU-8 grid dimensions ( $\mu\text{m}$ )	Expresses bidirectional system (Y/N)
200	N
300	N
400	N
500	N
600	Y
720	Y
800	Y

The SU-8 grids of smaller dimensions did not show much bidirectional folding, and in the warm state, the shapes curled up randomly, as can be seen in Figure 17. The bidirectional folding seemed to depend upon the aspect ratio of the SU-8 grids, the size of the grids and the spacing between them. It also seemed preferable to have anisotropically sized SU-8 grids, to encourage bidirectional folding.



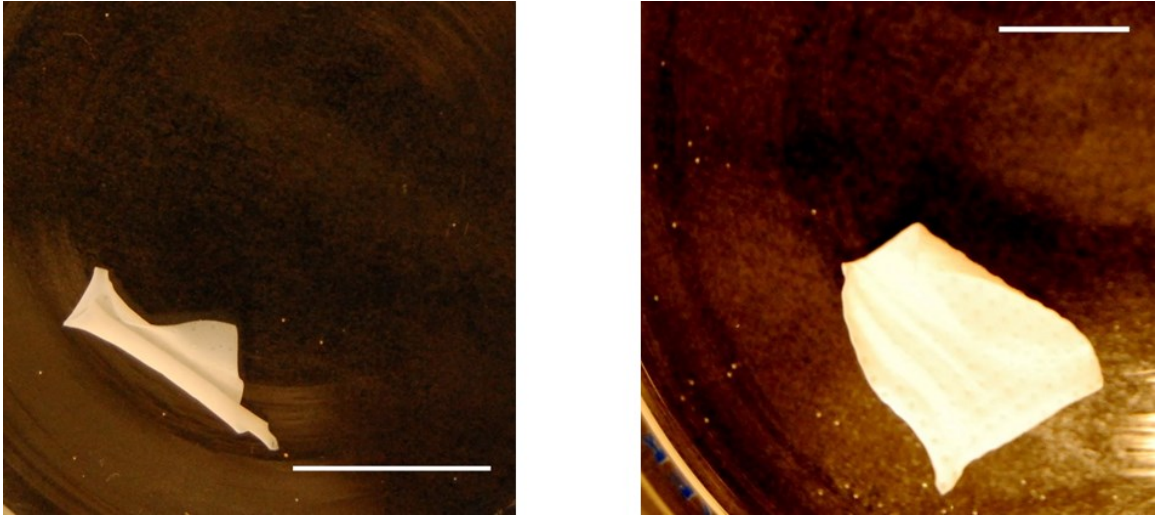


**Figure 17 - 200  $\mu\text{m}$  grids, the left figure shows the shape in the cold state, while the figure on the right shows the shape in the warm state, which exhibits uneven curling. Scale bars: 1 cm**

During the course of the experimentation, an observation was made that the SU-8 grids were slightly bent, which could be tending to bias the system into a more compact bidirectional folding in either states of the shape.

Images of this bending of a grid were taken using a microscope (NIKON AZ100 multi-zoom), by propping the shape against a wafer, placed vertically to get a magnified image on the side thickness of a grid. This has been shown below (Figure 17). MATLAB was used to characterize the radius of curvature of the grid, to quantify the extent of bending. This was 2.58 mm (+/- 0.43 mm). There also existed, a certain amount of saddling, which did not result in a completely flat structure when the shape is undergoing a transition at the transition temperature of the pNIPAM.

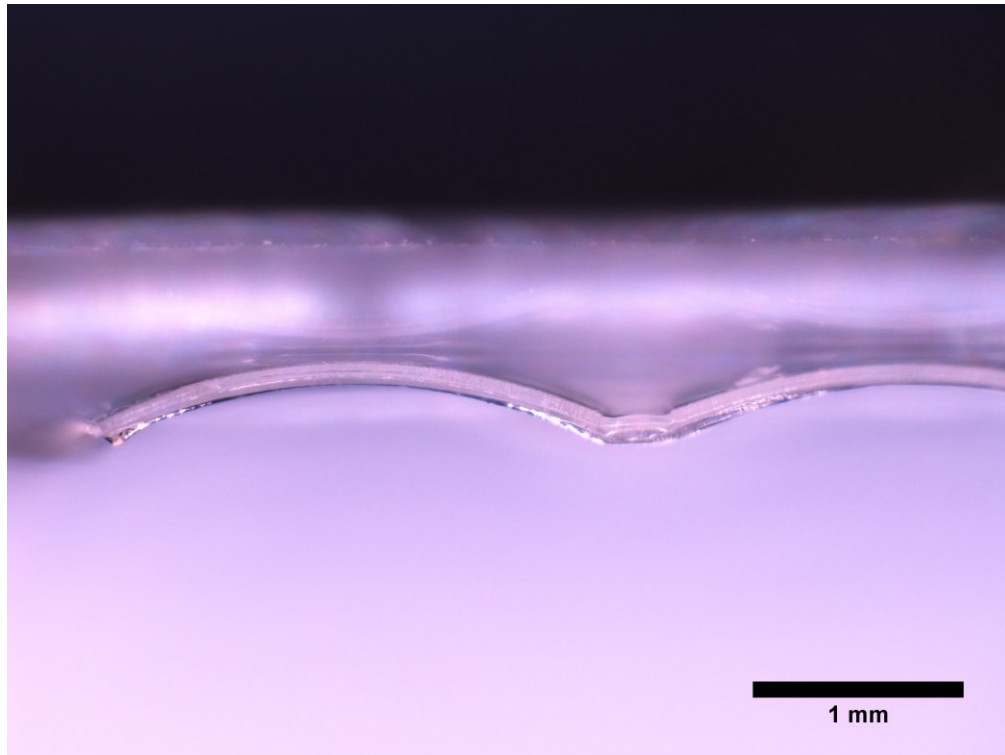


**Figure 18- Proof of bending in each grid of the hydrogel grid system**

Liu et al. have reported on observations like those in Figure 18. [96] Glassy polymers tend to absorb small amount of water and swell. In this paper, the authors created a cantilever of SU-8 and put a drop of water on the top. The SU-8 didn't have a crosslinking gradient due to exposure at  $500 \text{ mJ}/\text{cm}^2$ . They show that the capillary forces of the water drop to pull the cantilever towards it are not as strong because what is actually observed is that the cantilever tends to bend away from the water drop. This means that to some extent, the water molecules are diffusing through the SU-8, and since the drop was placed at the top of the cantilever, it diffused into the polymer network and caused the top region of the cantilever to swell and expand, thus pushing the beam downwards.

Schmid et al highlighted the effect of water absorption on the mechanical properties of SU-8, where the water absorbed by the SU-8 or other glassy polymers could enter the free voids in the polymer structure and increase the mass load, cause volume expansion and a modulus change.[97],[98],[99]

An article by Jamal et al showed how a crosslinking gradient in the SU-8 grids caused one region to swell more than the other and they used this to create self-folding microfluidics that were actuated by the presence of water.[30] The bending in the grids of the bidirectional folding hydrogel system could be reduced to a large extent by increasing the energy of UV exposure, and since the power from the UV lamp in the mask aligner is fixed, increasing the time of exposure can be the method to increase the energy of exposure. Hence, the total energy that the SU-8 grids were exposed to, to create an unbiased system with flat grids, was 500 mJ/cm<sup>2</sup>. The other method to create flat grids without a crosslinking gradient would be to use an alternative method to expose the sample through the bottom as well, if the substrate under the SU-8 layer could be glass instead of a silicon wafer. A situation like that could be simulated by positioning a reflective material directly below the SU-8 layer, to reflect the UV light back and aid the further crosslinking of the layer to eliminate the crosslinking gradient in the SU-8 layer. Gold is one such reflective material and has good adhesion to SU-8.[100]–[103] A protocol to attach a layer of gold to the SU-8 layer was tested, and indeed, the grids had a reduced crosslinking gradient.

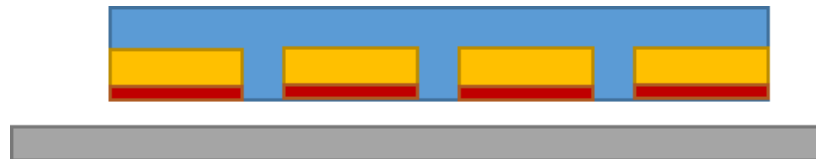


**Figure 19 - A visualization of the gold plated hydrogel - grid system, with respect to the silicon wafer (grey) in the absence of the sacrificial layer. The red layer below the yellow SU-8 layer is the gold layer, while the blue layer is the pNIPAM layer.**

## 2.4. Applications and Future Steps

Chun et al carried out studies on rectangular bilayers and observed a trend of the dependence of bending direction on aspect ratio.[92] They observed that bending tends to occur along the longer side of the rectangle and proved this by FEM modelling to show that strain energy was lowest in that case. Other observations have been made about rolling of rectangular strained films and trends recorded.[104] However, the reason for this low energy was not elaborated upon.

Observations have been made in thin rectangular bilayer films with one isotropically strained layer that they tend to bend along their long edges, and Alben et al explain the physical basis of this common phenomena.[91] They study bilayer systems made of polypyrrole (active film) and gold (passive substrate). The active film is actuated using a uniform strain, but being bonded to the substrate, it is restricted because both layers are to undergo the same amount of deformation. They state that a stretching energy of significant amount is required with films that are to curve in two orthogonal directions. Hence, they tend to curve along only one direction, and a rectangular shape can curl into a cigar, corkscrew or spiral shape. A rectangular bilayer tends to curl along its longer side and contains regions of double curvature, and this is due to a spatial distribution of curvatures. The magnitude of edge effects increases as the aspect ratio increases. The activation of the active film leads to the system bending and stretching, in and out of the plane. The energy associated with it involves stretching, bending and shear strain. They observe that the spiral shape has lower energy than cigar shape. They noted the experimental reasons for a particular configuration and hence chose materials that were polycrystalline or amorphous, and also stated that the prestressed sacrificial layer could be contributing to the constrained rolling.

Stoychev et al study the mechanics of folding in rectangular hydrogel bilayer systems.[38] They state how a rectangular bilayer can undergo three types of rolling, along the short side, long side or diagonals; edges of the hydrogel tend to absorb water and swell first, making hydrogels a heterogeneous active layer in a bilayer system. The passive layer in their system is PCL or PAA while the active layer is a thermoresponsive hydrogel, pNIPAM-AA-BA. The passive layers are hydrophobic and restrict the swelling of the hydrogel active layer. Photolithography was used to create the bilayers. They used the paper by Alben as a reference and stated similar observations (long side curling) in the case of narrower films, where the aspect ratio is high. The thickness range of the films is lower than one micron. They confirmed the observation that the diameter of the rolled up tubes depended mainly on thickness of the two layers and not so much on the dimensions of the rectangular systems. They state that swelling initially is diffusion controlled but over the long term, the final direction of swelling is controlled by adhesion of the bilayer system to the substrate.

Research has been done using shape changing hydrogel composite systems which can be differentially triggered by stimuli.[105] Various stimuli like pH, temperature, CO<sub>2</sub> supply, ionic strength were applied to a photolithographically “programmed” material composite to result a multi-responsive system. The system is essentially a semi-IPN of two hydrogels, where the first hydrogel (pNIPAM) is crosslinked, then soaked in the second hydrogel (PAMPS) before it is re-exposed to UV light through a mask, leading to the formation of an IPN with specifically programmed regions that are sensitive to different stimuli. Stimuli like a sodium chloride solution or increase in temperature caused the pNIPAM layer to collapse, and purging CO<sub>2</sub> into the system caused the PAMPS region to swell more than pNIPAM due to ionization upon decrease in the pH of the environment.

Miura ori patterns have widespread applications in fields involving compaction, like packing solar panels into small volumes so that when attached onto a satellite, they can be unfurled at the final site, and do not occupy too much space during the deployment process. Also, now 3-D transistors and lithium batteries are being investigated to create compact sources of power with a large power generating ability. Stimuli responsive panels are being investigated, which could be triggered by light to create electricity. This thermoresponsive system could find applications when triggered beyond the transition temperature of the pNIPAM to reveal the panels to either produce electricity or for thermoresponsive cargo offloading.[41], [81], [86], [106]–[115] Figures 19 and 20 show these applications.

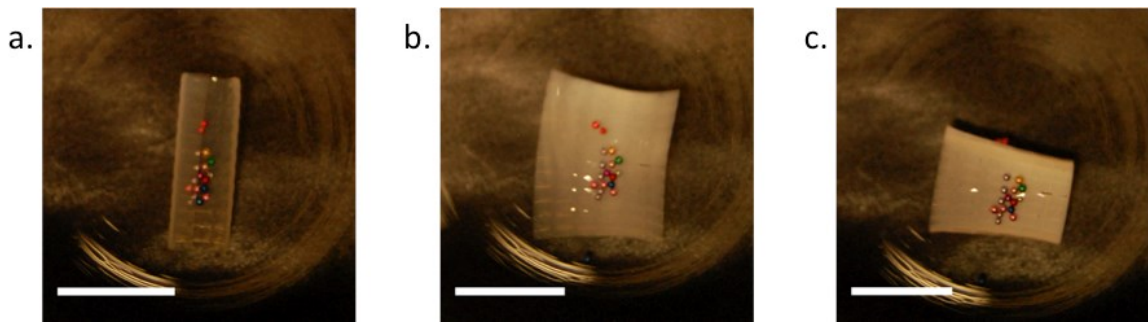


Figure 20 - The bidirectional folding system as a thermoresponsive cargo offloading device. Scale bar: 1 cm

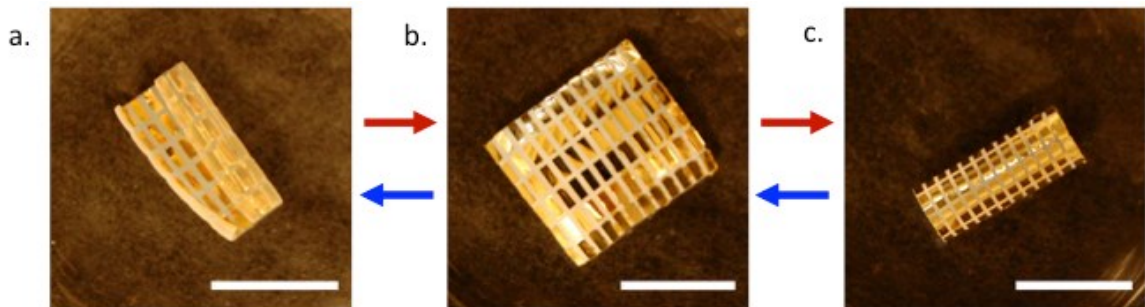


Figure 21 - The bidirectional folding system represented as a thermoresponsive photovoltaic. Scale bar: 1 cm.

Another interesting application of this system could be that of a temperature sensor. The flip could indicate the temperature of the medium surrounding the system.

Research by Madhukar et al investigates how a dome undergoing a large deformation tends to take many forms, and in some cases based on the thickness, there could exist a bistability that the dome experiences in the presence of a force along the axis of the dome.[111] This sort of a domed system has inspired the design of the device discussed in the following chapter. Upon further research into how to create the domed structures, photolithography has been used to create a hydrogel disc, restricted by a rim of a stiffer non swelling polymer, with materials similar to those used in this chapter.

## CHAPTER 3. SCOLEX-INSPIRED DRUG DELIVERY SYSTEM

### 3.1. Introduction

In this chapter, the thermoresponsive hydrogel and photoresist system has been studied in a different geometry, and an attempt has been made to create a self-folding drug delivery system inspired by gut parasites. A basic design of the system has been created using the existing swelling hydrogel-rigid polymer system, using a relevant geometry and a characterization study for dye release kinetics from the hydrogel was performed. This design could create an adhesive device that tends to pull the gut epithelium into it by means of creating a partial vacuum, as is in the case of gut parasites, and this has been elaborated upon in the future steps of the chapter. Additional ways to increase the adhesive tendency of this system were investigated, like adding a layer of a mucoadhesive polymer to the system using microfabrication. Also considered, were ways to make this system more biodegradable and biocompatible.

Drug delivery systems (DDSs) have evolved over the past decades to systems that release drugs in a controlled, sustained fashion.[116] The sustained drug delivery systems maintain a steady release of the drug and hence a steady supply of drug in the body which is essential to avoid the see-saw release profiles for DDSs showing burst release above and below the optimal amount of drug. The primary advantage of controlled drug delivery systems is better spatial and temporal bioavailability that minimizes the dosage of the drug to be administered and thus in turn reduced harmful side effects of the drug. They also improve patient compliance, by reducing the number of times a patient needs to take a dose of a drug. Thus it is essential for a drug release system to keep drug concentrations between the minimum effective concentration (MEC) and the maximum toxic concentration (MTC).[117]–



[119] A drug delivery system should contain the characteristics highlighted in Figure 22 below.[26], [120]

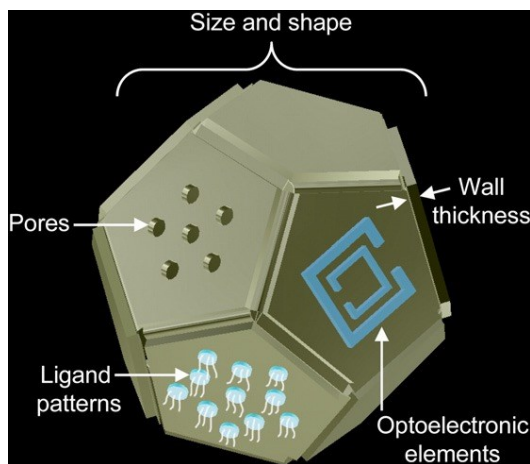


**Figure 22 - The components and characteristics of an effective drug delivery system. Reprinted with permission from Ref. [26] © 2012, Advanced Drug Delivery Reviews.**

Chemistry has evolved to create smart surfaces for controlled and sustained drug release through modifications of the material's structure, functionalization of the material surface or making the surface stimuli responsive.[20], [22] The system studied here is thermo-responsive and the room temperature to body temperature transition has been used to actuate the pNIPAM layer above 33°C. The pNIPAM layers tends to undergo a collapse above 33°C, where the hydrophobic interactions in the hydrogel dominate. Loading the hydrogel with drugs, could be a method to make it a drug delivery system, where the water and eventually the drug molecules could be released from the gel matrix above the transition temperature.

The inspiration for this project comes from gut parasites, which can remain embedded in the human gut for years on end. A literature search was conducted to study the various types of gut microbes in existence and the mechanisms that they use to survive in the varied environments in the human gastrointestinal tract.

The human body houses millions of organisms of sizes ranging from a few nanometers to over 10 meters.[121] The relationship between the body and these organism may be a symbiotic mutually beneficial one as in the case of commensals or of the type where only one side benefits, as in the case of a host and parasite.[122] The parasites are built to be able to draw nourishment and use various mechanisms to adhere within the host body. In some cases, gut commensals could turn into parasites.[123] Developing a drug delivery system that can adhere to the GI tract would involve a solid understanding of how these organisms adhere within the GI tract and how they manage to stay there for extended periods of time given the tendency of the gut epithelium to renew itself every few days. It is imperative to investigate biomaterials and methodologies that mimic the properties of body surfaces of the parasites which enable them to survive the wide pH variations in the GI tract ranging from a highly acidic pH in the stomach to a neutral to mildly basic pH as in the small and large intestines.

Drugs have been delivered in the GI tract using various pathways - rectal, buccal, nasal, ocular, vaginal, intravenous, and topical. The most convenient way to take the drug is orally in the form of a tablet or capsule[124], although oral drug delivery mechanisms have their fair share of challenges to overcome like varying pH in the GI tract, host immune response, low penetrability and constant renewal of the gut mucosa, etc. Drug delivery mechanisms can be tablets, capsules, intravenous delivery and patches or hydrogels that contain the drug.[125] Nanoparticles emerged as a new effective way to bypass the mucosa.[126] Larger drug molecules with a wide range of side effects that needed to be delivered in a controlled fashion require a different mode of delivery. Theragrippers are a drug delivery mechanism designed by the Gracias lab, seeking to overcome the challenge of the renewing mucosa by folding at the gut epithelium to “clamp” onto the gut wall. This would render them fixed at the site at which they are to deliver the medication.[127] During digestion, the muscles of the stomach

are constantly contracting and relaxing in peristaltic waves and thus, the theragrippers would allow for prolonged adhesion. The grippers are of the size of a few millimeters so that it is possible to take them orally. Enclosing them in a capsule casing would allow for prolonged survival without folding in the gut so that drug delivery could be extended to the small and large intestines. The material of construction of the new DDSs could be a pH sensitive material so as to let the pH of the environment trigger the folding of the grippers and hence decide the location to which the drug is to be delivered.[76] Temperature sensitivity of the gripper material, as is the current case, would be a useful mechanism for drug delivery in the stomach. Another factor to be considered is how far into the GI mucosa the DDSs must penetrate. The human mucosa is of varying thickness throughout the GI tract ranging from about 1500  $\mu\text{m}$  in the stomach to about 900  $\mu\text{m}$  in the rectum.[128]

*Helicobacter Pylori* is a commensal gut bacterium that could inspire a mechanism to would allow for the DDSs to survive the highly acidic pH of the stomach. The bacteria secretes urease which breaks down the stomach acid to release ammonia and carbon dioxide, allowing it just enough time to tunnel through the mucosa and find the submucosa of the gut.[129] *H. Pylori* is not an acidophile and hence can survive only in the depths of the mucosa, which can sustain an acidic pH on the side of the stomach lumen and a neutral environment on the side of the gut submucosa. The bacterium uses its polar flagella to tunnel through the mucosa and survives in high numbers up to 25 microns from the gastric epithelium. It can adhere to the epithelium using OMP (outer membrane proteins) adhesins to recognize specific glycoproteins of the host cells. This could inspire a new mechanism for targeted drug delivery especially in tumor recognition if the new DDSs were used to delivery cancer drugs.[130]

Pilli and fimbriae of bacteria provide a way of improving contact between the bacterium body and host cells.[131] This is seen in the case of E. Coli where the type 1 pilus of the bacterium in a broth culture would be about 1-2 microns in length while the length measured during E. Coli interactions with a host was about a tenth of that size.[132] This shows that the Pilli tend to contract upon contact with host cells, thus pulling the organism closer to the host cells, allowing for more intimate contact. This could be incorporated into the DDS design, but could be of a reversible fashion such that once the stipulated dose of the drug has been delivered, the system detaches and is washed out with the mucosa renews itself. This can be employed during delivery of drugs with major side effects that must be taken in small doses on a regular basis. It would be required that the DDSs adhere to the gut epithelium just long enough for the dose to be delivered, following which it detaches from the gut wall.

Another mechanism that would allow for detachment comes from parasites whose outermost layers of epithelium are shed away periodically so as to keep the host immune system at bay. Pills designed for controlled drug delivery encase a hydrogel, which contains an emulsion of the drug, which is exposed only as layers of the hydrogel begin to disintegrate.[58] Study of the tegument of Platyhelminthes gives an idea of how the parasite survives in the gut of the host.[133] The surface of the trematode is covered in covered in invaginations so as to increase surface area. There also exist spines and ridges of the size range of a few microns.

Parasites present in the gut of humans are larger in size than the micro-sized bacteria but they manage to effectively adhere and stay within the gut lumen for large periods of time. The study of mechanisms by which they achieve this could help enhance the DDS design. The physiology of trematodes shows that the tegument (cytoplasmic extension forming the outermost coating of the trematodes body which is about 15 microns thick) has an overall

negative charge due to a high concentration of sialic acid residues on the ends of the oligosaccharides that it is made up of.[134] Increasing hydrophilicity of the DDSs is essential so as to prevent too much interaction with the gut mucosa.[135] Trematodes adhere to the gut wall by means of suckers, which are cup shaped muscular organs made up of three types of muscles. The meridional muscles open the sucker while the equatorial and radial muscles (around the rim and on the inner and outer surfaces respectively) serve to create the cup shape of the closed sucker whose suction force causes a section of the gut wall tissue to be pulled into the sucker. This will inspire designs in the new DDS.

Bogitsh et al provide a broad overview on the endoparasites present in the human body.[136] Four classes of parasites make up the phylum Platyhelminthes – Trematoda, Cestoidea, Nematoda and Arthropoda. Within the trematoda class, liver flukes like *fasciola hepatica* could measure up to 30 mm in length and 13 mm in width, while intestinal flukes like *Fasciolopsis Buski* have dimensions of 75 mm by 20 mm. The main mode of attachment is the oral sucker, and in some cases, a ventral sucker. A collar of spines lines the side of the head in the case of *Echinostoma Trivolvis*. These are the main methods of attachment, along with enzymatic secretions by glands situated near the suckers, which cause lysis of tissue and allow the fluke body to be embedded more deeply and permanently within the host gut.

The class Cestoidea is different from Trematoda from the lack of a mouth and digestive tract. Eucestoda is the highly developed subclass, whose body consists of three regions – the scolex or head, the neck and the strobila. To facilitate attachment to the intestinal wall, scolices are employed. The most common scolex is the sucker, and the type of sucker determines the kind of scolex – acetabulate or bothriate. The acetabulate scolex comprises of four cups of muscular suckers, radially arranged around the scolex and equidistant, with a

rounded, oval or slit-like cup rim. An “armed” scolex has a line of hooks to aid attachment to the intestine wall. A bothriate scolex consists of depressions called bothria, which are longitudinally arranged. The scolices are also associated with secretions, to aid attachment and allow for the scolex to embed within the gut wall. The phylum Nematoda (roundworms) have elongated cylindrical bodies, tapered at both ends of length ranging from 1 mm to 15 cm. The mouth of the nematode opens into a buccal capsule, which could contain ridges, rods and plates, also, spears, teeth or stylets to aid attachment to the host tissue.

Understanding the physiology of mucus is essential to develop a drug delivery system that would make use of certain characteristics that might help it to adhere better to the mucus. An understanding of the chemistry involved is essential, and was covered extensively by Peppas and Sahlin.[137]

The design of the new scolex-inspired DDSs comprises of a disc of pNIPAM enclosed within a ring of SU-8 based on the paper by Sharon and Efrati[138] about a flat plate the insides of which undergo expansion. If the pNIPAM disc is unconstrained, it undergoes bending and can lead to a random shape. If the rim is constrained, the hydrogel will expand out of plane and will give a hemispherical shape as it swells. The rim of the feature was constrained with a non-swelling layer which stick to the swelling layer and this allows a controlled method of swelling. The thickness of the material is also known to play a role in the swelling characteristics.[139] The smaller is the thickness, higher is the chance of buckling energy to be the lower energy and hence the more favorable state of the disc. As stated by Klein et al, restrictions on a flat sheet can cause it to buckle, wrinkle or crumple.[140] They experimented with a new system of varying the crosslinking density of flat NIPA features and observing the contraction based on differential swelling in different radii to give variations in

the non-Euclidean surfaces created by the same flat configuration of the disc. Factors like crosslinking density, thickness of the plate, Gaussian curvature play an important role in deciding the value of  $K$  (curvature) to be positive or negative.

A very well studied model sucker presented is that of the octopus sucker, each sucker diameter being a few millimeters. There exist three kinds of muscles, meridional, circular and radial, just like in the tapeworm system, but the adhesion mechanism varies slightly, which can be better explained by the figure below.

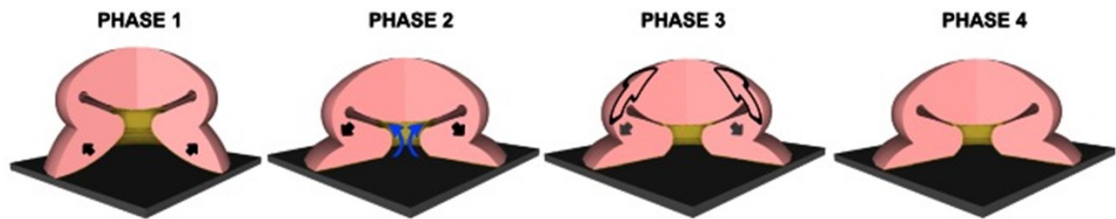


**Figure 23 - Adhesion mechanism of octopus suckers. . Reprinted from Ref. [141]© 2013, PLoS ONE.**

The hypothesis of the mechanism of adhesion of the sucker has been highlighted and mimicked by Kier et al.[142] The masks were designed trying to mimic these muscle orientations. Variation were made for circular muscles using a rim of SU-8 and spokes to mimic the radial muscles. The designs started with four spoke arrangements, radiating from the center of the circle. Other patterns later investigated included 6 spokes and disconnected spokes whose length is less than the radius of the circle. It is important to confine the pNIPAM gel within the boundaries of a rim of stiff non swelling material. Various reports on the muscle orientations of octopus suckers have been presented, and devices that mimicking this adhesive

action have been created, but on the macroscale, not using microfabrication.[141], [143]–[150]

The microfabrication of these devices has been described in the next section.

### **3.2. Fabrication and Experiments**

Microfabrication techniques like photolithography were used to create the suction cups in 2D. The fabrication procedure starts with the preparation of the stock solutions. This fabrication process is similar to section 2.2., for the fabrication of the bidirectional folding hydrogel system. For the sacrificial layer, a solution of 1:10 by weight of polyvinyl alcohol (PVA) in water was made. The photoresist SU-8 2025 for the non-swelling layer was obtained from Microchem and the poly(N-isopropyl acrylamide) stock solution for the swelling layer was prepared in accordance to the fabrication technique mentioned in the report by Bassik et al.[76] Briefly, a mixture was created, consisting of NIPAM monomer, some preexisting pNIPAM, BIS-acrylamide, 1-butanol, acrylic acid and the photoinitiator, Irgacure. This was covered in foil and stirred overnight at room temperature.

The photolithography was carried out in a clean room, where a 3 inch silicon wafer was rinsed first with acetone, then isopropyl alcohol (IPA), and then dried using a compressed nitrogen stream. This wafer was placed on a chuck in a spincoater and a small amount of PVA stock solution was dispensed on it using a disposable dropper. The wafer was then spun at 2000 rpm. This wafer was then placed on a hotplate at 115 °C for five minutes to dry.

Once dried and cooled to room temperature, the wafer was placed back in the spincoater and this time, a small amount of SU-8 2025 was added to the center of the wafer surface. Caution is to be exercised in not having any air bubbles trapped in this dispensed liquid, which could create an uneven surface during the spincoating step. The Microchem data



sheet very clearly states the procedure to handle the photoresist and pattern the resist, and the steps that have been mentioned below specifically relate to a particular spin speed and hence, a specific film thickness. The wafer with the SU-8 2025 was spun at 3000 rpm for a minute.

Once spun, the wafer was placed onto a hotplate at 65 °C for two minutes, followed by a hotplate at 95°C for five minutes and returned to the hotplate at 65°C for another two minutes. This is to ensure that the solvents in the resist layer thoroughly vaporized, and the resist layer was then dry. Once cooled to room temperature, the resist layer was manually checked to make sure it was dry, and if not, it was returned back to the 95°C hotplate for another two minutes. The temperature increment from 65 to 95°C is essential to not shock the resist. The resulting resist layer is 25 µm thick.

Upon returning the wafer to room temperature and once it is established that the SU-8 layer is thoroughly dried, the wafer was placed under a mask aligner (Quintel) and UV light was shined on it through a mask. The mask used is a negative mask, printed by Fineline Imaging. The clear regions of the mask directly exposed the resist to the UV light, which caused the resist to crosslink in those regions. The energy of exposure was 160 mJ/cm<sup>2</sup>. This was recommended by the Microchem data sheet for this thickness of the resist layer. Once exposed, the wafer was transferred back to the 66°C hotplate for one minutes, followed by five min at 95°C and one minute at 65°C. This post exposure baking step caused further crosslinking in the polymer network of the photoresist, while the UV light created the radicals in the resist, and initiated the polymerization. After the 1 minute on the 65°C hotplate, the features began to become more visible. Cooling to room temperature, the wafer was placed into an SU-8 developer solution (1-Methoxy-2-propyl acetate) until the unexposed regions of the photoresist dissolved completely. This took about 30 seconds, and the wafer was then

removed from the developer solution and washed for five seconds with acetone and then rinsed with copious amounts of IPA. The wafer was then dried using a nitrogen stream and placed into a petri dish in preparation for the next step of the fabrication procedure.

The next step in the fabrication procedure is to oxygen plasma treat the surface of the SU-8 features so as to make them more hydrophilic to allow for good adhesion between the pNIPAM layer and the SU-8 features. The wafers were placed into the plasma etch for 480 sec at 30 RF to clean the surface of the organic residue of the SU-8 developer, acetone and IPA. The treated wafer was then taken back to the cleanroom in preparation for the next layer to be added to it.

850  $\mu\text{l}$  of the pNIPAM stock solution are aliquoted onto the surface of the plasma treated wafer, and the wafer was swirled to let the stock solution coat the surface evenly. Once the stock solution was level on the surface of the wafer, the wafer was placed back in the mask aligner, but this time, non-contact lithography was performed, where the UV light was shined onto the wafer surface through a mask that did not touch the surface of the wafer. For this purpose, spacers were added to raise the mask slightly above the wafer surface, and UV light of  $60\text{mJ}/\text{cm}^2$  energy was shined on the pNIPAM layer. This layer was then washed with IPA to remove the uncrosslinked monomer solution, leaving behind the crosslinked pNIPAM layer in contact with the SU-8 layer. This was dried using a gentle stream of nitrogen to remove excess IPA. This bilayer was allowed to bond for four hours. The last step in the fabrication procedure was to add DI water to the petri dish containing the wafer, to dissolve the sacrificial layer and to liberate the features from the wafer, while at the same time allowing the pNIPAM layer to absorb the water and swell. The final feature was untethered and looked like that shown in Figure 24. Upon heating the water in which this shape was in, the cup tended to

collapse into a flat shape. These images have been captured using a NIKON AZ100 multi-zoom microscope.

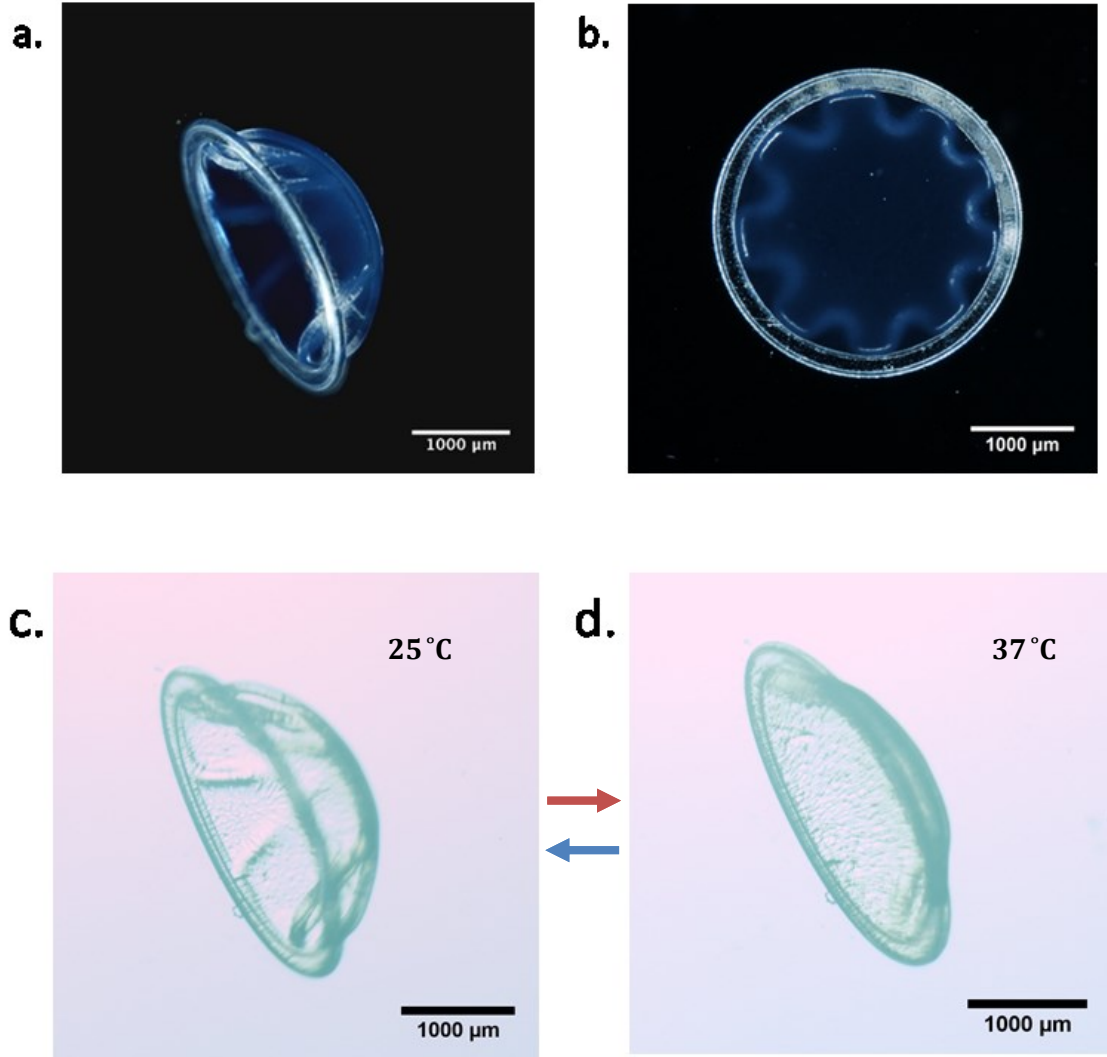
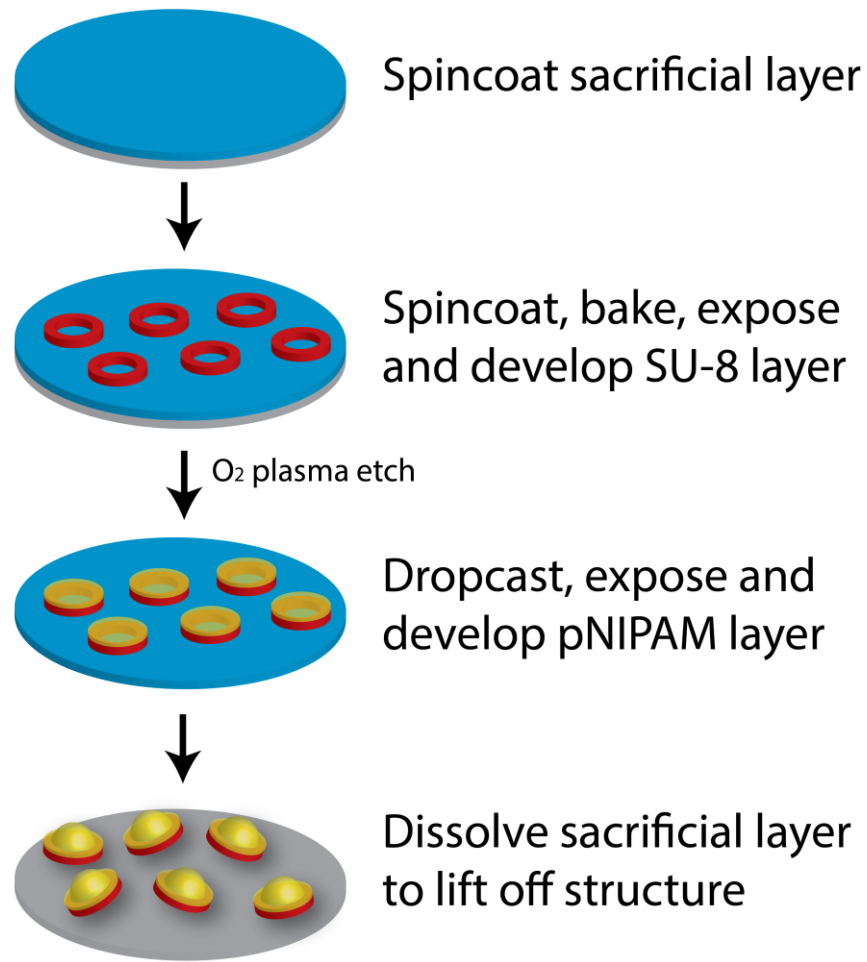


Figure 24 - An image of the suction cup, after the liftoff step of fabrication. (a.) A side view of the suction cup at room temperature, observed using bright field microscopy, (b.) the top view of the suction cup at room temperature, using bright field microscopy, (c.) side view of the room temperature suction cup, using fluorescence imaging (d.) Indicates the side view of the collapsed suction cup in warm water. The red arrow indicates warming while the blue arrow indicates cooling.

A schematic of the fabrication procedure for the suction cups has been shown in Figure 25.



**Figure 25 - Microfabrication schematic for the suction cups**

More geometries were created, to mimic the other muscle orientation of the scolex, using SU-8, the masks of which are shown below.

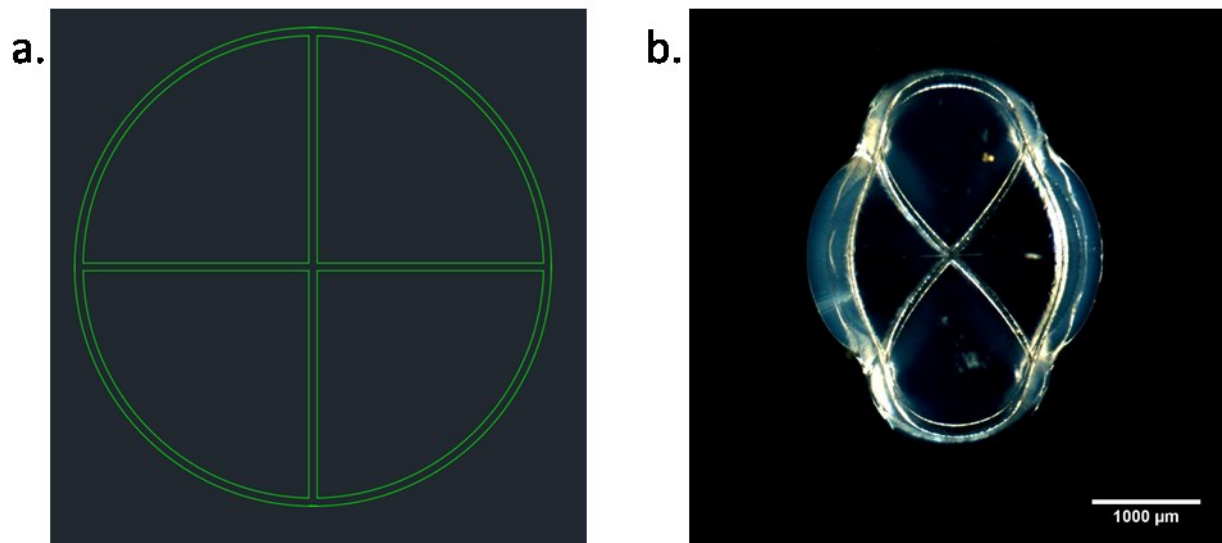


Figure 26 – (a.) Spokes in the SU-8 mask of 50  $\mu\text{m}$  thickness, (b.) The system after lift-off, once the pNIPAM layer is swollen.

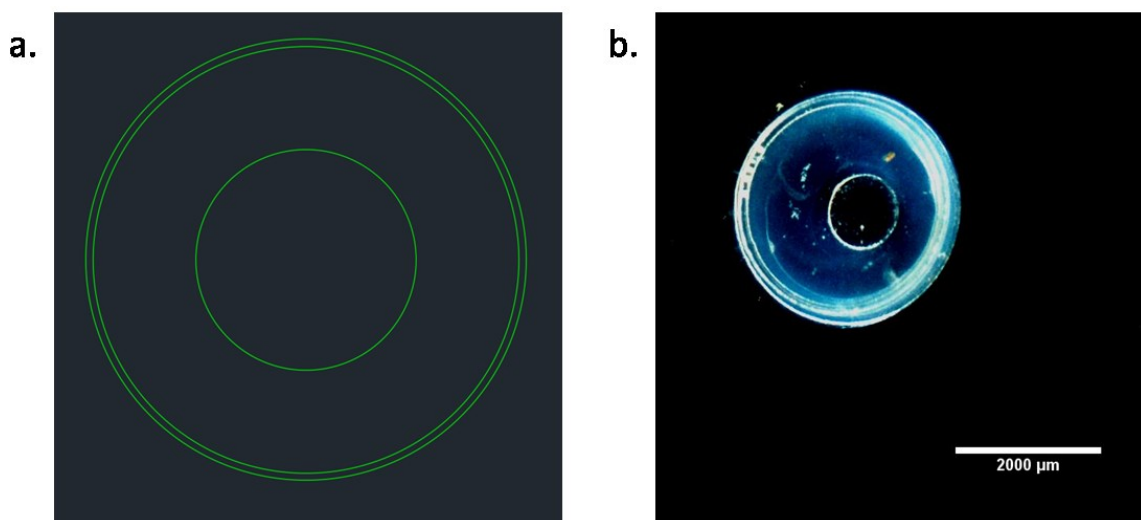
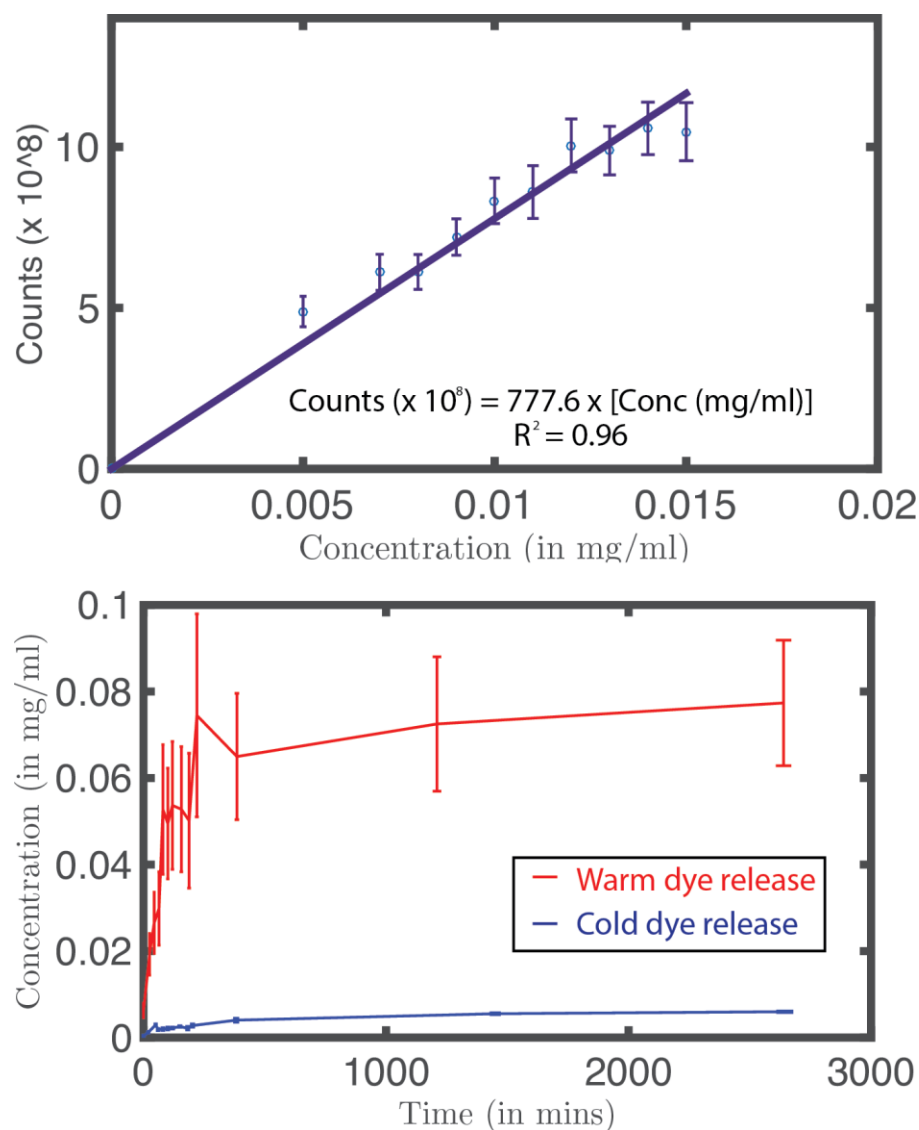


Figure 27 – (a.) A mask of another system of SU-8 mimicking the circular muscles, which contains a rim of SU-8 and a central patch of 200  $\mu\text{m}$  diameter. (b.) The system after lift-off, when the pNIPAM layer is swollen.

The dye release kinetics for this system were studied. This was in accordance to the protocol setup by Malachowski et al.[127] Five suction cups were soaked overnight in a solution of 1 mg/ml of fluorescein in water at room temperature. The dye would percolate

into the hydrogel mesh of the cups. These suction cups were then rinsed three times in DI water to rinse of dye particles that had not diffused into the hydrogel, and then transferred to a vial containing warm water at 40°C to mimic a body temperature environment. The group blank for this experiment was the same number of suction cups that were not soaked in fluorescein, placed into DI water at 40°C. The plate reader (Spectramax i3, Molecular Devices) also required there to be a plate blank, which was DI water at 40°C. At specific time intervals, aliquots of the sample were collected and diluted with DI water in a 96 well plate, along with a group and plate blank sample. The results have been collected as shown below. 4 trials of these readings were collected, over the span of 3 days. The control for this experiment was the release profile of five suction cups in DI water at room temperature. This system showed a lower release compared to the case where the hydrogel collapsed above transition temperature, as can be seen in Figure 28.



**Figure 28 - (Top)** The correlation between the fluorescence counts measured from the plate reader as a function of the concentration of fluorescein in mg/ml released into the warm water. **(Bottom)** The dye release studies for the suction cups in warm water in comparison to the control, of suction cups in water at room temperature.

After the final liftoff step of the suction cups from the wafer, an observation was made of a wrinkling pattern in the pNIPAM layer, just inside the SU-8 ring. This can be very noticeably observed in Figure 24. In this section, a small literature search has been conducted into wrinkling phenomena in similar systems to investigate potential causes of this. A product whose quality depends on a number of factors (parameters) needs to be systematically studied with the variation of each parameter.

### 3.3. Results and Discussions

A review by Dervaux and Amar extensively covers the range of mechanical instabilities that a hydrogel can undergo.[151] Based on the criteria stated by them, the issue at hand with our model is a wrinkle instability. The breakthrough work in this field was carried out by Tanaka et al.[152] The wrinkle formation occurs due to significant difference in the modulus of elasticity between the bilayers of the scolex.[153] It is also important to introduce some sort of strain to the system in the form of a stretch or heating or cooling (stretch is in this case). These wrinkles formed seem to be anisotropic (ordered).[154] Theory on the physics behind wrinkling deals with a tradeoff between bending resistance and longitudinal stretching near the region of constrain.[155] According to an article by Yang et al, when there is a confinement to a soft material at one end, it leads to anisotropic osmotic pressure across the lateral surface of the material.[156] Upon exceeding a critical value, the stress causes buckling of the surface. One way is to calculate the strain at the rim, which depends on the mechanical properties of the pNIPAM film (thickness and diameter of the layer).

This review by Chen and Yin[157] states that the mismatched deformation between the hydrogel film and less swelling substrate could be due to swelling mismatch or osmotic pressure and the film expands more than the substrate to render the film in a state of compression. When the stress is more than a threshold value, the film buckles. Two parameters to characterize buckling according to them is critical buckling stress and buckling wavelength. The stress driven buckling for spheroidal shapes has been characterized, using examples of fruits and vegetables.[158] A study about the propagation of tumors using a hydrogel model was able to characterize the mechanical instabilities of the system with relation to the physical properties and geometry of the system.[159] This system consisted of a central region of a lower swelling neutral hydrogel surrounded by a charged hydrogel ring of much



higher swelling capability. When the stiffness of the central region is less than that of the swelling gel, a buckling instability occurs wherein the boundaries of the swelling ring are nearly parallel. If the stiffness of the inner layer is greater than that of the swelling layer, creases begin to appear on the outer side of the ring while the inner side of the ring remains nearly circular. Wavelength dependence on thickness of the swelling layer helped to further quantify the instability. Another observation was a color gradient in the radial direction indicating that the gel swelled inhomogeneously.

In comparison, the system designed by us involves a stiff non swelling outer ring enclosing a swelling polymer hydrogel. The configuration is circular and hence similar to the article by Dervaux.[159] In some cases, the wrinkles seemed to lead to points of detachment.

This chapter discusses a new type of drug delivery system design which is inspired by gut parasite suckers. Their relevance as a drug delivery system was studied. An observation was made related to the mechanical instability of the hydrogel- polymer system which was characterized using a statistical method. A future direction of this research can be with the incorporation of a UCST expressing hydrogel and a mucoadhesive.[160], [161] Peppas and Sahlin reviewed the factors involved in developing a bioadhesive drug delivery system, and various methods to characterize the adhesiveness.[137] They focus on the polymers and the properties that make them mucoadhesive. Mortazavi and Smart investigated the factors developed a novel in vitro method to characterize mucoadhesiveness of a material by measuring the force involved and work done to detach a disc with mucoadhesive from a mucosa containing surface.[162]

Using the recipe from the report by Ahn et al. and by non-contact photolithography, a mucoadhesive was patterned as seen below.[163] For this purpose, Irgacure was introduced

as a crosslinking agent and the time of exposure, % chitosan and spincoating speed were decided empirically. Figure 29 highlights the results of patterning the novel mucoadhesive after spinning at 750 rpm for 10 seconds, followed by exposure to UV light with energy of 700 mJ/cm<sup>2</sup> through a mask, and rinsing off uncrosslinked monomer in an acetone bath for two minutes, followed by an IPA rinse and drying with a nitrogen stream.



**Figure 29 - Photopatterning a mucoadhesive based on chitosan and polyacrylic acid.**

Another consideration is to make the system biodegradable and biocompatible. pNIPAM and SU-8 to some extent can trigger cytotoxic responses in the body. Materials like chitosan, PLGA, cellulose and PHEMA can be investigated to improve the biodegradability of the system, and they also respond to various stimuli like pH and presence of ions in the water.[23], [64], [164], [165] A disadvantage of the controlled drug delivery system would be in the case of malfunction, if the bulk of the drug is dumped into the site of action of the DDS, called dose dumping, which could be dangerous in cases of drugs that have a small

difference between MEC and MTC. This also translates to reduced flexibility in administering the dose to a patient.[118]

The formulation of the pNIPAM stock solution can be altered to make it more and sensitive to stimuli like pH, temperature, even specific ions, electric field or magnetic field or even light.[76] Upon studying the collapse of the pNIPAM in warmer environments, it could be interesting to investigate the potential of this system as a valve that tends to push water forward in the direction of the collapse.

Further study needs to be carried out to address the above issues to make the suction cup system a viable, sustainable drug delivery mechanism.

## CHAPTER 4. SUMMARY AND FUTURE STEPS

In this thesis, a system comprising of a thermoresponsive hydrogel and a stiffer non-swelling component, in the presence of the temperature stimulus was studied and its different geometries explored. In particular, a certain geometry was shown to be capable of being used as a drug delivery system.

In the first part of the thesis, an observation was presented, where a thermoresponsive hydrogel sheet with stiff non-swelling polymer grids embedded in it underwent bidirectional folding upon collapse of the hydrogel induced by increasing the temperature. This bidirectional folding property was characterized by varying different parameters like number of grids, the rate of heating and cooling. A case was presented where the stiffer components had a crosslinking gradient and could be biasing the system. This challenge was overcome by eliminating the crosslinking gradient in the stiffer grid material by overexposure to UV light and the results of various cases of this hydrogel system were studied.

In Chapter 3, the hydrogel system was used with a different geometry to study a new type of drug delivery systems inspired by gut parasites. This system so far doesn't exhibit the partial vacuum creation property, however, methods were investigated to improve its tendency to adhere to the gut wall, one of them being to add a mucoadhesive layer. An observation related to the result of the fabrication, the mechanics of which were investigated, and the release kinetics of this system using a dye was studied.

This thesis can provide a platform to study the bidirectional folding aspects of a thermoresponsive hydrogel sheet with stiffer embedded grids, and to create a bio-inspired drug delivery system.

## REFERENCES

- [1] W. M. Moreau, *Semiconductor Lithography*. Boston, MA: Springer US, 1988.
- [2] P. Rai-Choudhury, *Handbook of microlithography, micromachining, and microfabrication*, vol. 1. 1997.
- [3] D. Brambley, B. Martin, and P. D. Prewett, "Microlithography: An overview," *Adv. Mater. Opt. Electron.*, vol. 4, no. 2, pp. 55–74, 1994.
- [4] W. P. Eaton and J. H. Smith, "Micromachined pressure sensors : review and recent developments," *Smart Mater. Struct.*, vol. 6, pp. 530–539, 1997.
- [5] G. T. A. Kovacs, K. Petersen, and M. Albin, "Peer Reviewed: Silicon Micromachining: Sensors to Systems," *Anal. Chem.*, vol. 68, no. 13, p. 407A–412A, 1996.
- [6] N. B. Bowden, M. Weck, I. S. Choi, and G. M. Whitesides, "Molecule-mimetic chemistry and mesoscale self-assembly," *Acc. Chem. Res.*, vol. 34, no. 3, pp. 231–238, 2001.
- [7] S. Alben and M. P. Brenner, "Self-assembly of flat sheets into closed surfaces," *Phys. Rev. E - Stat. Nonlinear, Soft Matter Phys.*, vol. 75, no. 5, pp. 1–8, 2007.
- [8] H. Cölfen and S. Mann, "Higher-order organization by mesoscale self-assembly and transformation of hybrid nanostructures," *Angew. Chemie - Int. Ed.*, vol. 42, no. 21, pp. 2350–2365, 2003.
- [9] M. Boncheva, D. a. Bruzewicz, and G. M. Whitesides, "Millimeter-scale self-assembly and its applications," *Pure Appl. Chem.*, vol. 75, no. 5, pp. 621–630, 2003.
- [10] C. Py, P. Reverdy, L. Doppler, J. Bico, B. Roman, and C. N. Baroud, "Capillary origami: Spontaneous wrapping of a droplet with an elastic sheet," *Phys. Rev. Lett.*, vol. 98, no. 15, pp. 2–5, 2007.
- [11] H. Li, X. Guo, R. G. Nuzzo, and K. Jimmy Hsia, "Capillary induced self-assembly of thin foils into 3D structures," *J. Mech. Phys. Solids*, vol. 58, no. 12, pp. 2033–2042, 2010.

- [12] T. G. Leong, B. R. Benson, E. K. Call, and D. H. Gracias, "Thin film stress driven self-folding of microstructured containers," *Small*, vol. 4, no. 10, pp. 1605–1609, 2008.
- [13] T. G. Leong, P. A. Lester, T. L. Koh, E. K. Call, and D. H. Gracias, "Surface tension-driven self-folding polyhedra," *Langmuir*, vol. 23, no. 17, pp. 8747–8751, 2007.
- [14] C. L. Randall, E. Gultepe, and D. H. Gracias, "Self-folding devices and materials for biomedical applications," *Trends Biotechnol.*, vol. 30, no. 3, pp. 138–146, 2012.
- [15] J. T. Santini, A. C. Richards, R. Scheidt, M. J. Cima, and R. Langer, "Microchips as controlled drug-delivery devices," *Angew. Chemie - Int. Ed.*, vol. 39, no. 14, pp. 2396–2407, 2000.
- [16] T. P. Richardson, M. C. Peters, a B. Ennett, and D. J. Mooney, "Polymeric system for dual growth factor delivery.," *Nat. Biotechnol.*, vol. 19, no. 11, pp. 1029–1034, 2001.
- [17] C. L. Randall, T. G. Leong, N. Bassik, and D. H. Gracias, "3D lithographically fabricated nanoliter containers for drug delivery," *Adv. Drug Deliv. Rev.*, vol. 59, no. 15, pp. 1547–1561, 2007.
- [18] I. I. Slowing, B. G. Trewyn, S. Giri, and V. S. Y. Lin, "Mesoporous Silica Nanoparticles for Drug Delivery and Biosensing Applications," *Adv. Funct. Mater.*, vol. 17, no. 8, pp. 1225–1236, 2007.
- [19] C. Boyer and J. A. Zasadzinski, "Serum," vol. 1, no. 3.
- [20] S. F. M. Van Dongen, H. P. M. De Hoog, R. J. R. W. Peters, M. Nallani, R. J. M. Nolte, and J. C. M. Van Hest, "Biohybrid polymer capsules," *Chem. Rev.*, vol. 109, no. 11, pp. 6212–6274, 2009.
- [21] S. P. Sullivan, D. G. Koutsonanos, M. Del Pilar Martin, J. W. Lee, V. Zarnitsyn, S.-O. Choi, N. Murthy, R. W. Compans, I. Skountzou, and M. R. Prausnitz, "Dissolving polymer microneedle patches for influenza vaccination.," *Nat. Med.*, vol. 16, no. 8, pp. 915–920, 2010.
- [22] B. Städler, A. D. Price, R. Chandrawati, L. Hosta-Rigau, A. N. Zelikin, and F. Caruso, "Polymer hydrogel capsules: en route toward synthetic cellular systems.," *Nanoscale*, vol. 1, no. 1, pp. 68–73, 2009.

- [23] S. K. Lai, J. S. Suk, A. Pace, Y. Y. Wang, M. Yang, O. Mert, J. Chen, J. Kim, and J. Hanes, "Drug carrier nanoparticles that penetrate human chronic rhinosinusitis mucus," *Biomaterials*, vol. 32, no. 26, pp. 6285–6290, 2011.
- [24] W. T. Al-Jamal and K. Kostarelos, "Liposomes: From a clinically established drug delivery system to a nanoparticle platform for theranostic nanomedicine," *Acc. Chem. Res.*, vol. 44, no. 10, pp. 1094–1104, 2011.
- [25] A. P. Esser-Kahn, S. A. Odom, N. R. Sottos, S. R. White, and J. S. Moore, "Triggered release from polymer capsules," *Macromolecules*, vol. 44, no. 14, pp. 5539–5553, 2011.
- [26] R. Fernandes and D. H. Gracias, "Self-folding polymeric containers for encapsulation and delivery of drugs," *Adv. Drug Deliv. Rev.*, vol. 64, no. 14, pp. 1579–1589, 2012.
- [27] L. Ionov, "Soft microorigami: self-folding polymer films," *Soft Matter*, vol. 7, no. 15, p. 6786, 2011.
- [28] J. C. Breger, C. Yoon, R. Xiao, H. R. Kwag, M. O. Wang, J. P. Fisher, T. D. Nguyen, and D. H. Gracias, "Self-folding thermo-magnetically responsive soft microgrippers," *ACS Appl. Mater. Interfaces*, vol. 7, no. 5, pp. 3398–3405, 2015.
- [29] C. Yoon, R. Xiao, J. Park, J. Cha, T. D. Nguyen, and D. H. Gracias, "Functional stimuli responsive hydrogel devices by self-folding," *Smart Mater. Struct.*, vol. 23, no. 9, p. 094008, 2014.
- [30] M. Jamal, A. M. Zarafshar, and D. H. Gracias, "Differentially photo-crosslinked polymers enable self-assembling microfluidics," *Nat. Commun.*, vol. 2, p. 527, 2011.
- [31] S. T. Brittain, O. J. a Schueller, H. K. Wu, S. Whitesides, and G. M. Whitesides, "Microorigami: Fabrication of small, three-dimensional, metallic structures," *J. Phys. Chem. B*, vol. 105, no. Figure 2, pp. 347–350, 2001.
- [32] E. Epstein, J. Yoon, A. Madhukar, K. J. Hsia, and P. V. Braun, "Colloidal Particles that Rapidly Change Shape via Elastic Instabilities," *Small*, vol. 11, no. 45, pp. 6051–6057, 2015.
- [33] L. Ionov, "Soft microorigami: self-folding polymer films," *Soft Matter*, vol. 7, no. 15, p. 6786, 2011.

- [34] J. Guan, H. He, D. J. Hansford, and L. J. Lee, "Self-folding of three-dimensional hydrogel microstructures," *J. Phys. Chem. B*, vol. 109, no. 49, pp. 23134–23137, 2005.
- [35] D. H. Gracias, "Stimuli responsive self-folding using thin polymer films," *Curr. Opin. Chem. Eng.*, vol. 2, no. 1, pp. 112–119, 2013.
- [36] D. H. Gracias, "Stimuli responsive self-folding using thin polymer films," *Curr. Opin. Chem. Eng.*, vol. 2, no. 1, pp. 112–119, 2013.
- [37] R. M. Erb, J. S. Sander, R. Grisch, and A. R. Studart, "Self-shaping composites with programmable bioinspired microstructures," *Nat. Commun.*, vol. 4, p. 1712, 2013.
- [38] G. Stoychev, S. Zakharchenko, S. Turcaud, J. W. C. Dunlop, and L. Ionov, "Shape-programmed folding of stimuli-responsive polymer bilayers," *ACS Nano*, vol. 6, no. 5, pp. 3925–3934, 2012.
- [39] Z. L. Wu, M. Moshe, J. Greener, H. Therien-Aubin, Z. Nie, E. Sharon, and E. Kumacheva, "Three-dimensional shape transformations of hydrogel sheets induced by small-scale modulation of internal stresses," *Nat. Commun.*, vol. 4, p. 1586, 2013.
- [40] L. Ionov, "Hydrogel-based actuators: Possibilities and limitations," *Mater. Today*, vol. 17, no. 10, pp. 494–503, 2014.
- [41] J. S. Randhawa, K. E. Laflin, N. Seelam, and D. H. Gracias, "Microchemomechanical systems," *Adv. Funct. Mater.*, vol. 21, no. 13, pp. 2395–2410, 2011.
- [42] E. Hawkes, B. An, N. M. Benbernou, H. Tanaka, S. Kim, E. D. Demaine, D. Rus, and R. J. Wood, "Programmable matter by folding," *Proc. Natl. Acad. Sci. U. S. A.*, vol. 107, no. 28, pp. 12441–5, 2010.
- [43] G. Stoychev, S. Turcaud, J. W. C. Dunlop, and L. Ionov, "Hierarchical multi-step folding of polymer bilayers," *Adv. Funct. Mater.*, vol. 23, no. 18, pp. 2295–2300, 2013.
- [44] K.-Z. Ivanić, Z. Tadić, and M. A. Omazić, "BIOMIMICRY – AN OVERVIEW," *Holist. Approach to Environ.*, vol. 5, no. 1, pp. 19–36, Mar. 2015.
- [45] R. Esfand and D. A. Tomalia, "Poly(amidoamine) (PAMAM) dendrimers: from biomimicry to drug delivery and biomedical applications," *Drug Discov. Today*, vol. 6, no. 8, pp. 427–436, Apr. 2001.



- [46] J. Braam, “In touch: Plant responses to mechanical stimuli,” *New Phytol.*, vol. 165, no. 2, pp. 373–389, 2005.
- [47] I. Burgert and P. Fratzl, “Actuation systems in plants as prototypes for bioinspired devices,” *Philos. Trans. R. Soc. A Math. Phys. Eng. Sci.*, vol. 367, no. 1893, pp. 1541–1557, 2009.
- [48] H. Lee, C. Xia, and N. X. Fang, “First jump of microgel; actuation speed enhancement by elastic instability,” *Soft Matter*, vol. 6, no. 18, p. 4342, 2010.
- [49] Y. Forterre, J. M. Skotheim, J. Dumais, and L. Mahadevan, “How the Venus flytrap snaps,” *Nature*, vol. 433, no. January, pp. 421–426, 2005.
- [50] M. J. Harrington, K. Razghandi, F. Ditsch, L. Guiducci, M. Rueggeberg, J. W. C. Dunlop, P. Fratzl, C. Neinhuis, and I. Burgert, “Origami-like unfolding of hydro-actuated ice plant seed capsules,” *Nat. Commun.*, vol. 2, no. May, p. 337, 2011.
- [51] Q. Ibrîm, T. M. Peakman, M. Biddle, C. Dawson, J. F. V Vincent, A.-M. Rocca, Q. Ibrîm, T. M. Peakman, and M. Biddle, “How pine cones open,” *Nat.*, vol. 390, no. 6661, p. 668, 1997.
- [52] L. Ionov, “Biomimetic hydrogel-based actuating systems,” *Adv. Funct. Mater.*, vol. 23, no. 36, pp. 4555–4570, 2013.
- [53] P. Fratzl and F. G. Barth, “Biomaterial systems for mechanosensing and actuation,” *Nature*, vol. 462, no. 7272, pp. 442–448, 2009.
- [54] S. Origami, “Self-Organized Origami,” vol. 307, no. March 2005, p. 2005, 2008.
- [55] P. Division, “Letters To Nature,” *Nature*, vol. 433, no. January, pp. 421–426, 2005.
- [56] D. P. Holmes and A. J. Crosby, “Snapping surfaces,” *Adv. Mater.*, vol. 19, no. 21, pp. 3589–3593, 2007.
- [57] A. Sidorenko, T. Krupenkin, A. Taylor, P. Fratzl, and J. Aizenberg, “Reversible Switching of Hydrogel-Actuated Nanostructures into Complex Micropatterns,” *Science (80-. )*, vol. 315, no. 5811, pp. 487–490, Jan. 2007.

- [58] A. S. Hoffman, “The origins and evolution of ‘controlled’ drug delivery systems,” *J. Control. Release*, vol. 132, no. 3, pp. 153–163, 2008.
- [59] P. Gupta, K. Vermani, and S. Garg, “Hydrogels: From controlled release to pH-responsive drug delivery,” *Drug Discov. Today*, vol. 7, no. 10, pp. 569–579, 2002.
- [60] I. Y. Galaev and B. Mattiasson, “‘Smart’ polymers and what they could do in biotechnology and medicine,” *Trends Biotechnol.*, vol. 17, no. 8, pp. 335–340, 1999.
- [61] F. Liu and M. W. Urban, “Recent advances and challenges in designing stimuli-responsive polymers,” *Prog. Polym. Sci.*, vol. 35, no. 1–2, pp. 3–23, 2010.
- [62] A. Lendlein and R. Langer, “Biodegradable, elastic shape-memory polymers for potential biomedical applications,” *Science*, vol. 296, no. 5573, pp. 1673–6, 2002.
- [63] A. Lendlein, M. Behl, B. Hiebl, and C. Wischke, “Shape-memory polymers as a technology platform for biomedical applications,” *Expert Rev. Med. Devices*, vol. 7, no. 3, pp. 357–379, 2010.
- [64] N. Bhattarai, J. Gunn, and M. Zhang, “Chitosan-based hydrogels for controlled, localized drug delivery,” *Adv. Drug Deliv. Rev.*, vol. 62, no. 1, pp. 83–99, 2010.
- [65] E. S. Matsuo and T. Tanaka, “Patterns In Shrinking Gels,” *Nature*, vol. 358, no. 6386, pp. 482–485, 1992.
- [66] S. Katayama, Y. Hirokawa, and T. Tanaka, “Reentrant phase transition in acrylamide-derivative copolymer gels,” *Macromolecules*, vol. 17, no. 12, pp. 2641–2643, 1984.
- [67] T. Tanaka, D. Fillmore, S.-T. Sun, I. Nishio, G. Swislow, and A. Shah, “Phase Transitions in Ionic Gels,” *Phys. Rev. Lett.*, vol. 45, no. 20, pp. 1636–1639, 1980.
- [68] P. J. Flory and J. Rehner, “Statistical Mechanics of Cross-Linked Polymer Networks II. Swelling,” *J. Chem. Phys.*, vol. 11, no. 11, p. 521, 1943.
- [69] S. Wongsuwarn, D. Vigolo, R. Cerbino, A. M. Howe, A. Vailati, R. Piazza, and P. Cicuta, “Giant thermophoresis of poly(N-isopropylacrylamide) microgel particles,” *Soft Matter*, vol. 8, p. 5857, 2012.

- [70] H. G. Schild, "Poly ( N-Isopropylacrylamide ): Experiment , Theory and Application," *Prog. Polym. Sci.*, vol. 17, pp. 163–249, 1992.
- [71] H. Mao, C. Li, Y. Zhang, D. E. Bergbreiter, and P. S. Cremer, "Measuring LCSTs by novel temperature gradient methods: Evidence for intermolecular interactions in mixed polymer solutions," *J. Am. Chem. Soc.*, vol. 125, no. 10, pp. 2850–2851, 2003.
- [72] A. Burmistrova, M. Richter, M. Eisele, C. Üzümlü, and R. von Klitzing, "The Effect of Co-Monomer Content on the Swelling/Shrinking and Mechanical Behaviour of Individually Adsorbed PNIPAM Microgel Particles," *Polymers (Basel)*, vol. 3, no. 4, pp. 1575–1590, 2011.
- [73] G. Yi, Y. Huang, F. Xiong, B. Liao, J. Yang, and X. Chen, "Preparation and swelling behaviors of rapid responsive semi-IPN NaCMC/PNIPAm hydrogels," *J. Wuban Univ. Technol. Mater. Sci. Ed.*, vol. 26, no. 6, pp. 1073–1078, 2011.
- [74] I. J. Suárez, A. Fernández-Nieves, and M. Márquez, "Swelling kinetics of poly(N-isopropylacrylamide) minigels," *J. Phys. Chem. B*, vol. 110, pp. 25729–25733, 2006.
- [75] A. Burmistrova, "Temperature-induced swelling / shrinking behavior of adsorbed PNIPAM microgels," 2011.
- [76] N. Bassik, B. T. Abebe, K. E. Laflin, and D. H. Gracias, "Photolithographically patterned smart hydrogel based bilayer actuators," *Polymer (Guildf)*, vol. 51, pp. 6093–6098, 2010.
- [77] M. R. G. Roelfsema and R. Hedrich, "In the light of stomatal opening: new insights into 'the Watergate'," *New Phytol.*, vol. 167, pp. 665–691, 2005.
- [78] P. T. Martone, M. Boiler, I. Burgert, J. Dumais, J. Edwards, K. MacH, N. Rowe, M. Rueggeberg, R. Seidel, and T. Speck, "Mechanics without Muscle: Biomechanical inspiration from the plant world," *Integr. Comp. Biol.*, vol. 50, no. 5, pp. 888–907, 2010.
- [79] R. Elbaum, L. Zaltzman, I. Burgert, and P. Fratzl, "The role of wheat awns in the seed dispersal unit," *Science*, vol. 316, no. 5826, pp. 884–886, 2007.
- [80] Y. Nishiyama, "Miura folding: applying origami to space exploration," *Int. J. Pure Appl. Math.*, vol. 79, no. 2, pp. 269–279, 2012.

- [81] J. L. Silverberg, A. A. Evans, L. McLeod, R. C. Hayward, T. Hull, C. D. Santangelo, and I. Cohen, “Applied origami. Using origami design principles to fold reprogrammable mechanical metamaterials,” *Science*, vol. 345, no. 6197, pp. 647–50, 2014.
- [82] T. Nojima, “Modelling of Folding Patterns in Flat Membranes and Cylinders by Using Origami,” *Transactions of the Japan Society of Mechanical Engineers Series C*, vol. 66, no. 643, pp. 1050–1056, 2000.
- [83] K. Kuribayashi, K. Tsuchiya, Z. You, D. Tomus, M. Umemoto, T. Ito, and M. Sasaki, “Self-deployable origami stent grafts as a biomedical application of Ni-rich TiNi shape memory alloy foil,” *Mater. Sci. Eng. A*, vol. 419, no. 1–2, pp. 131–137, 2006.
- [84] M. Schenk and S. D. Guest, “Geometry of Miura-folded metamaterials,” *Proc. Natl. Acad. Sci.*, vol. 110, no. 9, pp. 3276–3281, 2013.
- [85] J. L. Silverberg, J.-H. Na, A. A. Evans, B. Liu, T. C. Hull, C. D. Santangelo, R. J. Lang, R. C. Hayward, and I. Cohen, “Origami structures with a critical transition to bistability arising from hidden degrees of freedom,” *Nat. Mater.*, vol. 14, no. 4, pp. 389–393, 2015.
- [86] S. M. Felton, M. T. Tolley, B. Shin, C. D. Onal, E. D. Demaine, D. Rus, and R. J. Wood, “Self-folding with shape memory composites,” *Soft Matter*, vol. 9, no. 32, pp. 7688–7694, 2013.
- [87] S. Timoshenko, “Analysis of Bi-Metal Thermostats,” *J. Opt. Soc. Am.*, vol. 11, no. 3, p. 233, 1925.
- [88] Y. Liu, J. K. Boyles, J. Genzer, and M. D. Dickey, “Self-folding of polymer sheets using local light absorption,” *Soft Matter*, vol. 8, no. 6, p. 1764, 2012.
- [89] S. Turcaud, L. Guiducci, P. Fratzl, Y. J. M. Bréchet, and J. W. C. Dunlop, “An excursion into the design space of biomimetic architected biphasic actuators,” *Int. J. Mater. Res.*, vol. 02, pp. 4–9, 2011.
- [90] E. H. Mansfield, “Bending, Buckling and Curling of a Heated Elliptical Plate,” *Proc. R. Soc. A Math. Phys. Eng. Sci.*, vol. 288, no. 1414, pp. 396–417, Nov. 1965.
- [91] S. Alben, B. Balakrishnan, and E. Smela, “Edge effects determine the direction of bilayer bending,” *Nano Lett.*, vol. 11, no. 6, pp. 2280–2285, 2011.

- [92] I. S. Chun, A. Challa, B. Derickson, K. J. Hsia, and X. Li, "Geometry effect on the strain-induced self-rolling of semiconductor membranes," *Nano Lett.*, vol. 10, no. 10, pp. 3927–3932, 2010.
- [93] J. Kim, J. a. Hanna, R. C. Hayward, and C. D. Santangelo, "Thermally responsive rolling of thin gel strips with discrete variations in swelling," *Soft Matter*, vol. 8, no. 8, p. 2375, 2012.
- [94] L. T. De Haan, J. M. N. Verjans, D. J. Broer, C. W. M. Bastiaansen, and A. P. H. J. Schenning, "Humidity-responsive liquid crystalline polymer actuators with an asymmetry in the molecular trigger that bend, fold, and curl," *J. Am. Chem. Soc.*, vol. 136, no. 30, pp. 10585–10588, 2014.
- [95] B. Xu, H. Jiang, H. Li, G. Zhang, and Q. Zhang, "High strength nanocomposite hydrogel bilayer with bidirectional bending and shape switching behaviors for soft actuators," *RSC Adv.*, vol. 5, no. 17, pp. 13167–13170, 2015.
- [96] C. Liu, Y. Liu, M. Sokuler, D. Fell, S. Keller, A. Boisen, H.-J. Butt, G. K. Auernhammer, and E. Bonaccorso, "Diffusion of water into SU-8 microcantilevers," *Phys. Chem. Chem. Phys.*, vol. 12, no. 35, pp. 10577–83, 2010.
- [97] S. Schmid, S. Kühne, and C. Hierold, "Influence of air humidity on polymeric microresonators," *J. Micromechanics Microengineering*, vol. 19, no. 6, p. 065018, 2009.
- [98] G. C. Hill, R. Melamud, F. E. Declercq, A. A. Davenport, I. H. Chan, P. G. Hartwell, and B. L. Pruitt, "SU-8 MEMS Fabry-Perot pressure sensor," *Sensors Actuators, A Phys.*, vol. 138, no. 1, pp. 52–62, 2007.
- [99] V. M. Blanco Carballo, J. Melai, C. Salm, and J. Schmitz, "Moisture resistance of SU-8 and KMPR as structural material," *Microelectron. Eng.*, vol. 86, no. 4–6, pp. 765–768, 2009.
- [100] E. H. Conradie and D. F. Moore, "SU-8 thick photoresist processing as a functional material for MEMS applications," *J. Micromechanics Microengineering*, vol. 12, no. 4, pp. 368–374, 2002.
- [101] N. Chronis and L. P. Lee, "Total internal reflection-based biochip utilizing a polymer-filled cavity with a micromirror sidewall," *Lab Chip*, vol. 4, no. 2, pp. 125–30, 2004.
- [102] M. Nordstrom, A. Johansson, E. S. Nogueron, B. Clausen, M. Calleja, and A. Boisen,

- “Investigation of the bond strength between the photo-sensitive polymer SU-8 and gold,” *Microelectron. Eng.*, vol. 78–79, no. 1–4, pp. 152–157, 2005.
- [103] A. Rammohan, P. K. Dwivedi, R. Martinez-Duarte, H. Katepalli, M. J. Madou, and A. Sharma, “One-step maskless grayscale lithography for the fabrication of 3-dimensional structures in SU-8,” *Sensors Actuators, B Chem.*, vol. 153, no. 1, pp. 125–134, 2011.
- [104] P. Cendula, S. Kiravittaya, I. Mönch, J. Schumann, and O. G. Schmidt, “Directional roll-up of nanomembranes mediated by wrinkling,” *Nano Lett.*, vol. 11, no. 1, pp. 236–40, Jan. 2011.
- [105] H. Therien-Aubin, Z. L. Wu, Z. Nie, and E. Kumacheva, “Multiple shape transformations of composite hydrogel sheets,” *J. Am. Chem. Soc.*, vol. 135, no. 12, pp. 4834–4839, 2013.
- [106] C. Coupled, F. Quality, N. Release, Z. Author, J. U. Source, E. Society, A. S. Url, and U. T. C. R. Linked, “Linked references are available on JSTOR for this article : BY GRAZERS ’ ACTIVITIES : FOOD QUALITY,” vol. 74, no. 8, pp. 2337–2350, 2016.
- [107] J. P. Whitney, P. S. Sreetharan, K. Y. Ma, and R. J. Wood, “Pop-up book MEMS,” *J. Micromechanics Microengineering*, vol. 21, no. 11, p. 115021, 2011.
- [108] J. Ryu, M. D’Amato, X. Cui, K. N. Long, H. Jerry Qi, and M. L. Dunn, “Photo-origami-Bending and folding polymers with light,” *Appl. Phys. Lett.*, vol. 100, no. 16, 2012.
- [109] Q. Cheng, Z. Song, T. Ma, B. B. Smith, R. Tang, H. Yu, H. Jiang, and C. K. Chan, “Folding paper-based lithium-ion batteries for higher areal energy densities,” *Nano Lett.*, vol. 13, no. 10, pp. 4969–4974, 2013.
- [110] W. Wang, C. Yao, M.-J. Zhang, X.-J. Ju, R. Xie, and L.-Y. Chu, “Thermo-driven microcrawlers fabricated via a microfluidic approach,” *J. Phys. D. Appl. Phys.*, vol. 46, no. 11, p. 114007, 2013.
- [111] A. Madhukar, D. Perlitz, M. Grigola, D. Gai, and K. Jimmy Hsia, “Bistable characteristics of thick-walled axisymmetric domes,” *Int. J. Solids Struct.*, vol. 51, no. 14, pp. 2590–2597, 2014.

- [112] R. Tang, H. Huang, H. Tu, H. Liang, M. Liang, Z. Song, Y. Xu, H. Jiang, and H. Yu, "Origami-enabled deformable silicon solar cells," *Appl. Phys. Lett.*, vol. 104, no. 8, pp. 2012–2017, 2014.
- [113] C. Ye and V. V Tsukruk, "Designing two-dimensional materials that spring rapidly into three-dimensional shapes," *Science (80-. )*, vol. 347, pp. 130–131, 2015.
- [114] J. R. Cooke, "Deployable Structures and Biological Morphology," *6th Int. Conf. Comput. Shell Spat. Struct.*, p. 21, 2008.
- [115] S. Zakharchenko, N. Pureskiy, G. Stoychev, M. Stamm, and L. Ionov, "Temperature controlled encapsulation and release using partially biodegradable thermo-magneto-sensitive self-rolling tubes," *Eur. Cells Mater.*, vol. 20, no. SUPPL.3, p. 279, 2010.
- [116] R. S. Langer, "New Methods of Drug Delivery," *Science (80-. )*, vol. 249, no. 4976, pp. 1527–1533, 1990.
- [117] W. M. Saltzman, *Drug Delivery: Engineering Principles for Drug Therapy*. Oxford University Press, 2001.
- [118] M. D. Kutmalge, A. N. Jadhav, M. P. Ratnaparkhi, and S. P. Chaudhari, "SUSTAINED RELEASE DRUG DELIVERY SYSTEM," *PHARMA Sci. Monit.*, vol. 5, no. 2, pp. 21–38, 2014.
- [119] S. I. Shen, B. R. Jasti, and X. Li, "Design Of Controlled Release Drug Delivery Systems," *Stand. Handb. Biomed. Eng. Des.*, pp. 1–14, 2004.
- [120] T. M. Allen and P. R. Cullis, "Drug Delivery Systems : Entering the Mainstream," *Science (80-. )*, vol. 303, no. 5665, pp. 1818–1822, 2004.
- [121] J. Howell and G. Brown, "Education and imaging. Gastrointestinal: beef tapeworm (*Taenia saginata*).," *J. Gastroenterol. Hepatol.*, vol. 23, no. 11, p. 1769, Nov. 2008.
- [122] F. Guarner, "Gut flora in health and disease," *Lancet*, vol. 381, 2003.
- [123] M. S. Gilmore and J. J. Ferretti, "Microbiology. The thin line between gut commensal and pathogen.," *Science*, vol. 299, no. 5615, pp. 1999–2002, 2003.

- [124] I. Vhora, S. Patil, and P. Bhatt, "Protein and Peptide Drug Delivery," *Protein Pept. Nanoparticles Drug Deliv.*, pp. 1–55, 2015.
- [125] D. A. LaVan, T. McGuire, and R. Langer, "Small-scale systems for in vivo drug delivery," *Nat. Biotechnol.*, vol. 21, no. 10, pp. 1184–1191, 2003.
- [126] S. K. Lai, Y.-Y. Wang, and J. Hanes, "Mucus-penetrating nanoparticles for drug and gene delivery to mucosal tissues," *Adv. Drug Deliv. Rev.*, vol. 61, no. 2, pp. 158–171, 2009.
- [127] K. Malachowski, J. Breger, H. R. Kwag, M. O. Wang, J. P. Fisher, F. M. Selaru, and D. H. Gracias, "Stimuli-Responsive Theragrippers for Chemomechanical Controlled Release.," *Angew. Chem. Int. Ed. Engl.*, pp. 1–6, 2014.
- [128] C. H. Huh, M. S. Bhutani, E. B. Farfán, and W. E. Bolch, "Individual variations in mucosa and total wall thickness in the stomach and rectum assessed via endoscopic ultrasound.," *Physiol. Meas.*, vol. 24, no. 4, pp. N15–N22, 2003.
- [129] M. R. Amieva and E. M. El-Omar, "Host-Bacterial Interactions in Helicobacter pylori Infection," *Gastroenterology*, vol. 134, no. 1, pp. 306–323, 2008.
- [130] M. Gladwin and B. Trattler, *Clinical microbiology made ridiculously simple*. 2003.
- [131] K. A. Kline, S. F?lker, S. Dahlberg, S. Normark, and B. Henriques-Normark, "Bacterial Adhesins in Host-Microbe Interactions," *Cell Host Microbe*, vol. 5, no. 6, pp. 580–592, 2009.
- [132] M. A. Mulvey, Y. S. Lopez-boado, C. L. Wilson, R. Roth, C. William, J. Heuser, and S. J. Hultgren, "Induction and Evasion of Host Defenses by Type 1-Piliated Uropathogenic Escherichia coli Author(s): Matthew A. Mulvey, Yolanda S. Lopez-Boado, Carole L. Wilson, Robyn Roth, William C . Parks, John Heuser and Scott J. Hultgren Source:," vol. 282, no. 5393, pp. 1494–1497, 2016.
- [133] G. Gobert and D. Stenzel, "The ultrastructural architecture of the adult Schistosoma japonicum tegument," *Int. J. ...*, 2003.
- [134] J. D. Smyth and D. W. Halton, *the physiology of Trematodes*. Science, 1983.
- [135] H. H. Sigurdsson, J. Kirch, and C. M. Lehr, "Mucus as a barrier to lipophilic drugs,"



*Int. J. Pharm.*, vol. 453, no. 1, pp. 56–64, 2013.

- [136] B. J. Bogitsh, C. E. Carter, and T. N. Oeltmann, *Human Parasitology*. 2013.
- [137] N. A. Peppas and J. J. Sahlin, “Hydrogels as mucoadhesive and bioadhesive materials: A review,” *Biomaterials*, vol. 17, no. 16, pp. 1553–1561, 1996.
- [138] E. Sharon and E. Efrati, “The mechanics of non-Euclidean plates,” *Soft Matter*, vol. 6, no. 22, p. 5693, 2010.
- [139] E. Efrati, E. Sharon, and R. Kupferman, “Elastic theory of unconstrained non-Euclidean plates,” *J. Mech. Phys. Solids*, vol. 57, no. 4, pp. 762–775, Apr. 2009.
- [140] Y. Klein, E. Efrati, and E. Sharon, “Shaping of elastic sheets by prescription of non-Euclidean metrics,” *Science*, vol. 315, no. 5815, pp. 1116–20, Feb. 2007.
- [141] F. Tramacere, L. Beccai, M. Kuba, A. Gozzi, A. Bifone, and B. Mazzolai, “The Morphology and Adhesion Mechanism of Octopus vulgaris Suckers,” *PLoS One*, vol. 8, no. 6, p. e65074, Jun. 2013.
- [142] W. M. Kier and A. M. Smith, “The structure and adhesive mechanism of octopus suckers,” *Integr. Comp. Biol.*, vol. 42, no. 6, pp. 1146–53, Dec. 2002.
- [143] F. W. Grasso and P. Setlur, “Inspiration, simulation and design for smart robot manipulators from the sucker actuation mechanism of cephalopods,” *Bioinspir. Biomim.*, vol. 2, no. 4, pp. S170–S181, Dec. 2007.
- [144] F. Tramacere, L. Beccai, F. Mattioli, E. Sinibaldi, and B. Mazzolai, “Artificial adhesion mechanisms inspired by octopus suckers,” in *2012 IEEE International Conference on Robotics and Automation*, 2012, pp. 3846–3851.
- [145] F. Tramacere, A. Kovalev, T. Kleinteich, S. N. Gorb, and B. Mazzolai, “Structure and mechanical properties of Octopus vulgaris suckers,” *J. R. Soc. Interface*, vol. 11, no. 91, pp. 20130816–20130816, Nov. 2013.
- [146] H. Bing-shan, W. Li-wen, F. Zhuang, and Z. Yan-zheng, “Bio-inspired Miniature Suction Cups Actuated by Shape Memory Alloy,” *Int. J. Adv. Robot. Syst.*, vol. 6, no. 3, 2009.

- [147] C. C. Kessens and J. P. Desai, “Design, fabrication, and implementation of self-sealing suction cup arrays for grasping,” in *2010 IEEE International Conference on Robotics and Automation*, 2010, pp. 765–770.
- [148] M. Follador, F. Tramacere, and B. Mazzolai, “Dielectric elastomer actuators for octopus inspired suction cups,” *Bioinspir. Biomim.*, vol. 9, no. 4, p. 046002, Sep. 2014.
- [149] P. R. Bandyopadhyay, J. D. Hrubes, and H. A. Leinhos, “Biorobotic adhesion in water using suction cups,” *Bioinspir. Biomim.*, vol. 3, no. 1, p. 016003, Mar. 2008.
- [150] F. Tramacere, L. Beccai, and B. Mazzolai, “What Can We Learn from the Octopus?,” in *Biological and Biomimetic Adhesives*, Cambridge: Royal Society of Chemistry, pp. 89–102.
- [151] J. Dervaux and M. Ben Amar, “Mechanical Instabilities of Gels,” *Annu. Rev. Condens. Matter Phys.*, vol. 3, no. 1, pp. 311–332, Mar. 2012.
- [152] T. Tanaka, S.-T. Sun, Y. Hirokawa, S. Katayama, J. Kucera, Y. Hirose, and T. Amiya, “Mechanical instability of gels at the phase transition,” *Nature*, vol. 325, no. 6107, pp. 796–798, Feb. 1987.
- [153] F. S. Teixeira, M. C. Salvadori, W. W. R. Araújo, H. J. M. Amorim, M. Cattani, and I. G. Brown, “Isotropic and anisotropic wrinkling of diamond-like carbon films on polydimethylsiloxane substrates,” *J. Appl. Phys.*, vol. 113, no. 23, p. 234904, Jun. 2013.
- [154] N. Bowden, S. Brittain, A. G. Evans, J. W. Hutchinson, and G. M. Whitesides, “Spontaneous formation of ordered structures in thin films of metals supported on an elastomeric polymer,” vol. 393, no. 6681, pp. 146–149, May 1998.
- [155] E. Cerda, K. Ravi-Chandar, and L. Mahadevan, “Thin films. Wrinkling of an elastic sheet under tension,” *Nature*, vol. 419, no. 6907, pp. 579–80, Oct. 2002.
- [156] S. Yang, K. Khare, and P.-C. Lin, “Harnessing Surface Wrinkle Patterns in Soft Matter,” *Adv. Funct. Mater.*, vol. 20, no. 16, pp. 2550–2564, Aug. 2010.
- [157] X. Chen and J. Yin, “Buckling patterns of thin films on curved compliant substrates with applications to morphogenesis and three-dimensional micro-fabrication,” *Soft Matter*, vol. 6, no. 22, p. 5667, Nov. 2010.

- [158] J. Yin, Z. Cao, C. Li, I. Sheinman, and X. Chen, "Stress-driven buckling patterns in spheroidal core/shell structures.," *Proc. Natl. Acad. Sci. U. S. A.*, vol. 105, no. 49, pp. 19132–5, Dec. 2008.
- [159] J. Dervaux, Y. Couder, M.-A. Guedeau-Boudeville, and M. Ben Amar, "Shape transition in artificial tumors: from smooth buckles to singular creases.," *Phys. Rev. Lett.*, vol. 107, no. 1, p. 018103, Jul. 2011.
- [160] K. Ono, Y. Saito, H. Yura, K. Ishikawa, A. Kurita, T. Akaike, and M. Ishihara, "Photocrosslinkable chitosan as a biological adhesive," *J. Biomed. Mater. Res.*, vol. 49, no. 2, pp. 289–295, 2000.
- [161] J. D. Smart, "The basics and underlying mechanisms of mucoadhesion," *Adv. Drug Deliv. Rev.*, vol. 57, no. 11, pp. 1556–1568, 2005.
- [162] S. A. Mortazavi and J. D. Smart, "An investigation of some factors influencing the in vitro assessment of mucoadhesion," *Int. J. Pharm.*, vol. 116, no. 2, pp. 223–230, 1995.
- [163] J. S. Ahn, H. K. Choi, and C. S. Cho, "A novel mucoadhesive polymer prepared by template polymerization of acrylic acid in the presence of chitosan," *Biomaterials*, vol. 22, no. 9, pp. 923–928, 2001.
- [164] X. Qiu and S. Hu, "'Smart' materials based on cellulose: A review of the preparations, properties, and applications," *Materials (Basel)*, vol. 6, no. 3, pp. 738–781, 2013.
- [165] T. S. Shim, S. H. Kim, C. J. Heo, H. C. Jeon, and S. M. Yang, "Controlled origami folding of hydrogel bilayers with sustained reversibility for robust microcarriers," *Angew. Chemie - Int. Ed.*, vol. 51, no. 6, pp. 1420–1423, 2012.

## CURRICULUM VITAE

JOHNS HOPKINS UNIVERSITY  
3400 N. Charles St., Baltimore, MD 21218

**TANVI SHROFF**

Phone: (443)255-5860  
Email: [shroff@jhu.edu](mailto:shroff@jhu.edu)

---

### EDUCATION

- **M.S.E. (Thesis based), Chemical and Biomolecular Engineering** *Aug 2014 – May 2016*  
Johns Hopkins University (J.H.U.), Baltimore, MD. **GPA: 3.80/4.0**
- **B.E., Chemical Engineering** *Aug 2010 – May 2014*  
Institute of Chemical Technology (I.C.T.), Mumbai, India. **GPA: 8.62/10.0**  
**Senior Design Project** – Designed a manufacturing facility complete with a P&ID diagram for the manufacture of 100 tons per day of glycerol carbonate, a biodegradable solvent, derived from glycerol.
  - Award: Acharya P. C. Ray award for 2<sup>nd</sup> best Senior Design Project, I.C.T. 2014

### RESEARCH and WORK EXPERIENCE

- **Graduate researcher, Gracias Laboratory, J.H.U.** *Aug 2014 – Present*  
**Advisors:** Dr. David Gracias (Department of Chemical and Biomolecular Engineering), Dr. Thao Nguyen (Department of Mechanical Engineering), Dr. Florin Selaru (Johns Hopkins Hospital).  
**Thesis:** Microfabricated Dynamic Shape-Change Hydrogel Systems
- **Summer Intern, Sandoz, India** *Summer, 2013*
- **Research Assistant, I.C.T.** *May 2012 – Jan 2014*
- **Summer Intern, Standard Engineers Pvt. Ltd., India** *Summer, 2011*

### PUBLICATIONS

- *Shroff, Yoon, Gracias. Shape Change Poly(N-Isopropylacrylamide) Microstructures for Drug Delivery, Aldrich Material Science, 2015; pp. 28. (<http://goo.gl/F4y5HN>)*
- *Reversible Bidirectional Folding of a Hydrogel System* *(In submission)*

### LEADERSHIP AND TEACHING EXPERIENCE

- **Teaching Assistant, J.H.U.** *Jan 2016 – Present*  
**COURSE** – “Advanced Chemical Reaction Engineering in Practice”, **Course Director:** Dr. Pereira
- **Teaching Assistant, J.H.U.** *Aug 2015 – Dec 2015*  
**COURSE** – “Dynamic Modeling and Control”, **Course Director:** Dr. An Goffin
- **Mentor, Women in Science and Engineering (WISE) program, J.H.U.** *Aug 2015 – Feb 2016*  
Mentor to 2 students from Garrison Forest High School, working to create 2-D structures that fold into complex 3-D origami.

### RESEARCH EXPERIENCE

- **Microfabrication** – Photolithography, Cleanroom protocols, soft lithography, vapor deposition, 3-D printing
- **Biological material handling** – Sterile/ aseptic laboratory techniques like cell culture, Plate readers for absorbance and fluorescence
- **Software** – AutoCAD, Adobe Illustrator, Microsoft Office, MATLAB, Design of Experiments
- **Imaging** – Scanning Electron microscopy, Optical and Fluorescence microscopy.

LinkedIN - [goo.gl/3D7Ol3](http://goo.gl/3D7Ol3)